Metabolic Engineering 91 (2025) 276–289

Contents lists available at ScienceDirect

Metabolic Engineering

journal homepage: www.elsevier.com/locate/meteng

Beyond CEN.PK - parallel engineering of selected *S. cerevisiae* strains reveals that superior chassis strains require different engineering approaches for limonene production

Yanmei Zhu [a,b], Sasha Yogiswara [a,b], Anke Willekens [a,b], Agathe Gérardin [a,b], Rob Lavigne [c], Alain Goossens [d,e,f], Vitor B. Pinheiro [g], Zongjie Dai [h,*], Kevin J. Verstrepen [a,b,**]

[a] *VIB – KU Leuven Center for Microbiology, Gaston Geenslaan 1, 3001, Leuven, Belgium*
[b] *CMPG Laboratory of Genetics and Genomics, Department M2S, KU Leuven, Gaston Geenslaan 1, 3001, Leuven, Belgium*
[c] *Laboratory of Gene Technology, KU Leuven, Kasteelpark Arenberg 21 box 2462, Heverlee, 3001, Leuven, Belgium*
[d] *Department of Plant Biotechnology and Bioinformatics, Ghent University, B-9052 Ghent, Belgium*
[e] *VIB Center for Plant Systems Biology, B-9052 Ghent, Belgium*
[f] *Department of Botany and Zoology, Stellenbosch University, Private Bag X1, Matieland, 7600, South Africa*
[g] *KU Leuven, Rega Institute for Medical Research, Department of Pharmaceutical and Pharmacological Sciences, Herestraat, 49 – box 1041, 3000, Leuven, Belgium*
[h] *Key Laboratory of Engineering Biology for Low-carbon Manufacturing, Tianjin Institute of Industrial Biotechnology, Chinese Academy of Sciences, Tianjin, 300308, China*

ARTICLE INFO

Keywords:
Microbial cell factory
Chassis strain
Saccharomyces cerevisiae
Limonene
Mevalonate pathway
Precision fermentation

ABSTRACT

Genetically engineered microbes are increasingly utilized to produce a broad range of high-value compounds. However, most studies start with only a very narrow group of genetically tractable type strains that have not been selected for maximum titers or industrial robustness. In this study, we used high-throughput screening and parallel metabolic engineering to identify and optimize *Saccharomyces cerevisiae* chassis strains for the production of limonene, a monoterpene with applications in flavors, fragrances, and biofuels. We screened 921 genetically and phenotypically distinct *S. cerevisiae* strains for limonene tolerance and lipid content to identify optimal chassis strains for precision fermentation of limonene. In parallel, we also evaluated 16 different plant limonene synthases. Our results revealed that two of the selected strains showed approximately a 2-fold increase in titers compared to CEN.PK2-1C, the type strain that is often used as a chassis for limonene production, with the same genetic modifications in the mevalonate pathway. Intriguingly, the most effective engineering strategy proved strain-specific. Metabolic profiling revealed that this difference is likely explained by differences in native mevalonate production. Ultimately, by using strain-specific engineering strategies, we achieved 844 mg/L in a new strain, 40 % higher than the titer (605 mg/L) achieved by CEN.PK2-1C. Our findings demonstrate the potential of leveraging genetic diversity in *S. cerevisiae* for monoterpene bioproduction and highlight the necessity for tailoring metabolic engineering strategies to specific strains.

1. Introduction

Microbial cell factories provide a promising route towards a more sustainable bio-based economy with reduced use of fossil and animal resources. Although certain high-value compounds are already successfully produced by microbial cell factories (Liu et al., 2024; Rehm and Wibowo, 2022; Zhang et al., 2022), many other compounds synthesized in laboratory settings have yet to be implemented at an industrial scale because the titers and yields are not economically viable. Hence, attention in the field is shifting from pathway engineering towards the optimization of yield and titer. For example, new techniques to optimize expression levels in complex pathways or achieve higher titers through adaptive laboratory evolution are being developed (Cautereels et al., 2024a, 2024b; Konzock and Nielsen, 2024; Mavrommati et al., 2022; Montano Lopez et al., 2022; Zimmermann et al., 2023, 2024). Despite the progress in molecular technologies, the potential of selecting

* Corresponding author.
** Corresponding author. VIB – KU Leuven Center for Microbiology, Gaston Geenslaan 1, 3001 Leuven, Belgium.
E-mail addresses: daizj@tib.cas.cn (Z. Dai), kevin.verstrepen@kuleuven.be (K.J. Verstrepen).

https://doi.org/10.1016/j.ymben.2025.04.011
Received 17 January 2025; Received in revised form 29 April 2025; Accepted 30 April 2025
Available online 5 May 2025

different chassis microbes to increase titers remains underexplored. Most research is conducted in a limited number of type strains that have been selected for their tractability, but not for their performance towards a specific industrial process. Previous research demonstrated that different isolates of some of the most-used industrial microbes show remarkable phenotypic diversity, with large innate differences in stress tolerance and metabolite production (Gallone et al., 2016, 2019; Kong et al., 2018; Monk et al., 2016; Mukherjee et al., 2014). We therefore hypothesized that the selection of more optimal chassis strains may, in some cases, enable substantial improvements in performance and titers.

Saccharomyces cerevisiae is emerging as one of the most important chassis for the biosynthesis of valuable compounds, owing to its well-characterized genetic background and the availability of sophisticated genetic editing tools (Botstein and Fink, 2011; Chen et al., 2018; Siddiqui et al., 2012). Several studies have uncovered the immense genetic and phenotypic diversity within *S. cerevisiae* (Gallone et al., 2016, 2019; Liti et al., 2009; Loegler et al., 2024; Peter et al., 2018) and highlighted that type strains often perform sub-optimally in industrially-relevant conditions. For example, high-throughput characterization of large libraries of *S. cerevisiae* strains has identified new variants suited for bioethanol (Mukherjee et al., 2014), beer (Steensels et al., 2014a), cocoa (Meersman et al., 2013, 2016) and wine (Granchi et al., 2019; Romano et al., 2008) fermentations. While strategies for engineering industrial *S. cerevisiae* strains have been explored, and a handful industrial *S. cerevisiae* strains have been engineered for e.g. monoterpenes production (Denby et al., 2018), ergosterol synthesis (Sun et al., 2021), amino acids biosynthesis (Hu et al., 2025), enhanced tolerance to environmental stresses (Wan et al., 2024) and improved lignocellulose inhibitor resistance (Brandt et al., 2021), and C5 sugar utilization (Duperray et al., 2024; Feng et al., 2018), it is still not well understood whether and to what extent the extraordinary biodiversity within the *S. cerevisiae* species can be exploited to find new chassis strains for precision fermentation.

Here, we explore the intraspecific diversity of *S. cerevisiae* to identify superior chassis strains for precision fermentation. The biosynthesis of limonene, a monoterpene used as a fragrance and food-flavoring compound, was used as a case study (Anandakumar et al., 2021; Ciriminna et al., 2014; Ibanez et al., 2020; Miller et al., 2010; Vieira et al., 2018). Current production methods for limonene involve chemical extraction from fruit peels, which imposes a high environmental cost and shows only limited efficiency (Negro et al., 2016; Paggiola et al., 2016). Production in microbes provides a more sustainable alternative (Jongedijk et al., 2016; Ren et al., 2020). Like most monoterpenes, limonene is toxic to yeast cells (Brennan et al., 2012, 2013; Liu et al., 2013), and this negatively impacts cell growth and product yield. Cytotoxicity is a major obstacle to large-scale production of limonene and its derivatives in microbial systems (Jongedijk et al., 2016). To mitigate product toxicity, key strategies include the overexpression of efflux pumps (Demissie et al., 2019; Hu et al., 2012), compartmentalization engineering (Bernard et al., 2024; Dusseaux et al., 2020), adaptive laboratory evolution (Li et al., 2024), and two-phase fermentation (Bernard et al., 2024; Brennan et al., 2012; Cheng et al., 2019; Dusseaux et al., 2020; Ignea et al., 2019; Kong et al., 2023; Zhang et al., 2021). However, studies screening high-monoterpene-tolerant chassis strains for the hyperproduction of related products are rarely reported.

S. cerevisiae is particularly attractive for producing plant-derived terpenoids due to its endogenous mevalonate (MVA) pathway, which supplies essential precursors (Leavell et al., 2016; Westfall et al., 2012). Some of the highest sesquiterpenoid titers achieved so far have been reported in *S. cerevisiae*, including 28.3 g/L for farnesene (Wang et al., 2023) and 25 g/L for artemisinic acid (Paddon et al., 2013). However, titers for monoterpenes remain much lower, despite efforts to enhance MVA pathway flux, optimize the expression of rate-limiting synthases, redirect farnesyl pyrophosphate (FPP) flux towards monoterpene biosynthesis, mitigate cytotoxic effects, optimize substrate utilization, and refine fermentation processes (Li et al., 2024). For example, the highest reported titer for limonene in *S. cerevisiae* in optimized fed-batch fermentation is 4.2 g/L (Su et al., 2024), followed by 2.6 g/L (Kong et al., 2023), 2.2 g/L (Zhang et al., 2021), and 1.0 g/L (Peng et al., 2022). Additionally, most efforts have focused on optimizing metabolic engineering and fermentation strategies, and these have all been limited to only a few type strains, such as CEN.PK2-1C (Bernard et al., 2024; Cheah et al., 2023; Cheng et al., 2019; Kong et al., 2023; Peng et al., 2022; Zhang et al., 2021), S288C (Zhou et al., 2023), and W303 (Dusseaux et al., 2020).

In this study, we explored the potential of a broad range of *S. cerevisiae* strains as sustainable chassis for limonene production. To identify superior chassis strains, we screened a large collection of *S. cerevisiae* strains (921 strains from 12 ecological niches, including several domesticated strains used in different industrial processes). Specifically, we screened for limonene tolerance and acetyl-CoA provision, a key monoterpene precursor, via lipid content. We also investigated 16 different limonene synthases and showed that the synthase *CltLS1* from *Citrus limon* is the optimal limonene synthase for limonene production in *S. cerevisiae*. Parallel genetic engineering of different *S. cerevisiae* strains selected for increased limonene tolerance or lipid content revealed that different strains undergoing the same engineering strategies showed vastly different limonene titers, with the titers of the most commonly used chassis strains being inferior to those of the best isolates. Moreover, optimal engineering strategies were strain-dependent. Ultimately, strain Y243, a strain originating from the baking industry, proved to be a superior chassis for limonene production. With strain-specific engineering approaches, it produced 40 % more limonene compared to CEN.PK2-1C, which is the most frequently used chassis strain for limonene production so far. Comparative metabolomics revealed that mevalonate level is a determining factor in superior limonene production of different *S. cerevisiae* chassis strains.

2. Materials and methods

2.1. Strains and growth media

A total of 921 *Saccharomyces cerevisiae* strains, including three type strains (CEN.PK2-1C, S288C, W303), used in this study (Table S1) were obtained from the in-house VIB collection. Strains were inoculated from glycerol stock (2 % [wt/vol] Bacto peptone, 1 % [wt/vol] yeast extract, 2 % [wt/vol] glucose, 25 % [wt/vol] glycerol), stored at −80 °C, and plated on yeast extract peptone dextrose (YPD) 2 % agar plates (2 % [wt/vol] Bacto peptone, 1 % [wt/vol] yeast extract, 2 % [wt/vol] agar, 2 % [wt/vol] glucose) using a ROTOR robot (Singer Instruments), and strains were grown at 25 °C until colonies were visible (up to 3 days). For testing, colonies were grown in YPD 2 % (2 % Bacto peptone, 1 % yeast extract, 2 % glucose) medium, unless extra antibiotics were required for the selection of constructs (100 μg/mL Hygromycin (Life Technologies, 10687010) or 100 μg/mL clonNAT (Jena Bioscience, AB-102L). *Escherichia coli* DH5α, which was used for plasmid construction and amplification, was grown in Lysogeny Broth (LB) medium (1 % peptone, 1 % NaCl, 0.5 % yeast extract) at 37 °C. When needed, the media was supplemented with 100 μg/mL of Carbenicillin (Labconsult bvba, DUC. C0109.0005) or 50 μg/mL of Kanamycin (Sigma, K4000).

2.2. High-throughput screening for limonene tolerance and lipid content

To assess the effect of limonene on yeast growth, all 921 yeast strains were inoculated into 150 μL of YPD 2 % in 96-well plates, and strains were grown at 25 °C with 600 rpm shaking for 72 h on a plate shaker. Next, pre-growth cultures were diluted into fresh 150 μL of YPD 2 % in a new 96-well plate to OD600–0.01 (considered as time 0). Then, 10 % [vol/vol] *n*-dodecane (Thermo Scientific, 117590025) containing varying concentrations of limonene (Sigma-Aldrich, 62118) was added to the culture. The two-phase culture system was cultivated at 25 °C for 48 h shaking at 150 rpm. Growth (OD600) was measured by a Tecan

Infinite plate reader. Based on preliminary tests, 300 mM limonene (concentration in dodecane) was selected as the concentration for the first round of screening. Then, 500 mM, 1000 mM, and 1500 mM were used to select more limonene-tolerant strains, and this selection was carried out in triplicates.

To assess the lipid content of the strains, all 921 yeast strains were first cultivated in 150 μL of SD (synthetic defined, 0.17 % YNB (Yeast Nitrogen base: without amino acid and ammonium sulfate), 0.077 % CSM (Complete Supplement Mixture), 0.5 % ammonium sulfate, 2 % glucose) medium in 96-well plates at 25 °C with 600 rpm for 48 h. Next, the cultures were diluted into 150 μL of NLSD (nitrogen-limited SD, 0.17 % YNB (without amino acid and ammonium sulfate), 0.077 % CSM, 0.1 % ammonium sulfate, 2 % glucose) (Shi et al., 2016) in a 96-well plate to OD600–0.01 (considered as time 0), grown at 25 °C with 600 rpm for 72 h. After that, cellular growth (OD600) and fluorescence (580 nm) were measured by a Tecan Infinite plate reader. For the Nile red staining, 125 μL of cell culture was transferred to a black 96-well plate and 25 μL of 0.05 mg/mL Nile red (Sigma Aldrich, 19123-10 MG) solution (in dimethyl sulfoxide, DMSO (VWR, 23500.297)) was added. Initial fluorescence excitation was set at 485/25 nm, with emission at 535/35 nm, and kinetic readings were performed for 10 min with 60-s intervals following the method described by (Sitepu et al., 2012). The optical position on the Tecan reader was set to the top 50 %, and maximal emission values were determined.

2.3. PCR, cloning, and gene synthesis

Primers used for sequence amplification, integration, and verification were ordered from Integrated DNA Technologies (IDT), and primer sequences are listed in Table S2. Gene constructs were amplified using PrimeSTAR GXL DNA polymerase (TaKaRa). DNA amplification from the colony was first done by boiling the colony in NaOH at 99 °C and then by PCR using Sapphire AmpFast PCR mix (Takara Bio). Plasmid pV1382 (Addgene Plasmid #111436), which encodes the Cas9 protein, was used as a backbone to express sgRNA. Most plasmids used in this study were constructed using Gibson Assembly (NEBuilder HiFi DNA Assembly Master Mix) and several plasmids were ordered from Addgene (Table S3). Plasmid purification was performed using the QIAprep Spin Miniprep Kit (Qiagen). Sanger sequencing was used to confirm constructs and genes generated and it was performed by Eurofins Genomics.

The coding sequence (CDS) of nine limonene synthases (LSs) (*CutLS1*, *CutLS2*, *CltLS1*, *CltLS2*, *CltLS3*, *CstLS*, *PttLS*, *ArtLS*, and *ShtLS*) was taken from Cheng et al. (2019). The CDS of the remaining seven LSs (*MptLS*, *TstLS*, *LatLS*, *CatLS*, *SdtLS*, *PctLS*, and *SttLS*) were downloaded from NCBI, and NCBI accession numbers can be found in Table S4. N-terminal domains were removed and the CDS were codon-optimized for *S. cerevisiae* (IDT Codon Optimization Tool). The 16 CDSs were combined with strong promoters (P_{TDH3}) and terminators (T_{CYC1}) to create expression constructs which were flanked by 200 bp homology to ARS308a loci at each end, to allow for genomic integration. These 16 constructs were synthesized by Qinglan Biotech, BGI (sequences can be found in Table S5).

2.4. Ploidy and cell size determination of strains

To determine the ploidy of strains, yeast cells were inoculated into 1 mL YPD 2 % medium in a 96-well plate and incubated overnight at 30 °C on a plate shaker (600 rpm). The next day, cells were collected by centrifugation (3000 rpm, 3 min), washed with 1 mL deionized water (dH_2O), centrifuged again, and resuspended in 750 μL 70 % [vol/vol] ethanol. Plates were sealed with a silver seal and incubated for at least 16 h at 4 °C. On day three, cells were first centrifuged (3000 rpm, 3 min), and pellets were resuspended in 500 μL SC-buffer (0.007 % [wt/vol] citric acid, 1.46 % [wt/vol] sodium citrate). Then cells were centrifuged again and resuspended in 1 mL SC-buffer containing 0.25 mg/mL RNase A (Thermo Scientific, #AB-0549; pre-boiled at 95 °C for 5 min). Plates were sealed and incubated for 1 h at 50 °C. Next, 50 μL Proteinase K (Thermo Scientific, #BP1700-100; 20 mg/mL in SC-buffer) was then added, followed by an additional 1-h incubation at 50 °C. Cells were centrifuged, washed with 500 μL SC-buffer, resuspended in 1 mL SC-buffer, and stained with propidium iodide (Sigma, #P4864-10 ML) at a final concentration of 16 μg/mL. Plates were resealed (protected from light) and incubated for at least 16 h at 4 °C. On day four, samples were washed with 1 mL sodium citrate solution, resuspended in 750 μL of the same buffer, and analyzed on an Attune NxT Flow Cytometer (Thermo Scientific). Propidium iodide fluorescence was detected using the BL2 laser (excitation: 488 nm), with standard settings (flow rate: 100 μL/min; acquisition volume: 200 μL; total number of events: 50,000 events/sample).

To measure the cell size, yeast cells were inoculated into 1 mL YPD 2 % medium in a 96-well plate and incubated overnight at 30 °C. Then 10 μL cell culture was transferred to a new plate and diluted in 190 μL Attune™ Focusing Fluid (1X). Samples were analyzed by Attune NxT Flow Cytometer (Thermo Scientific) using the BL2 laser with standard settings (same as above) and the median of FSC-A was calculated. Microscopy images of strains were taken using a Nikon ECLIPSE Ti microscope equipped with a 100 × oil immersion objective lens and a 10 × ocular lens, and image scales were added in ImageJ.

2.5. Strain transformation and construction

All gene constructs (listed in Table 1 and Table S3) were placed under constitutive promoters and flanked by 50–200 bp homology arms targeting the genomic integration sites. Each gene construct was integrated into the genomic integration site (Table S6) for stable expression, and integration sites were chosen based on a study by Reider et al., 2017. Gene constructs were integrated via CRISPR-Cas9 (Reider Apel et al., 2017), and a list of gRNAs targeting the different integration sites can be found in Table S6. Yeast transformation was carried out using a DMSO-LiAc procedure (Pan et al., 2004), and for some industrial strains, an electroporation protocol (as described in (Thompson et al., 1998)) was used to make the transformation more efficient. All the engineered strains are listed in Table S7.

2.6. Two-phase batch fermentation

For fermentation, single colonies were picked from the YPD 2 % agar plate and inoculated into 3 mL of YPD medium and cultivated at 30 °C, with 250 rpm agitation overnight. Subsequently, the seed culture was transferred into 20 mL glass vials with magnetic screw caps containing 10 mL of YPD 2 % medium with an initial OD600 of 0.2. The two-phase fermentation was started by adding 10 % [vol/vol] dodecane as the organic extractant phase into vials. The mixture was then incubated at 30 °C, 200 rpm for 48 h on a magnetic stirring platform (2mag stirring drive MIXdrive 60). At the end of the fermentation period (48 h), vials were chilled at 4 °C for 1 h before collecting the dodecane layer by centrifugation at 4500 rpm for 10 min. Limonene concentrations in dodecane were then measured as described below and are presented in

Table 1
Letter of gene constructs used for labeling engineered strains.

Letter	Gene construct
A	P_{TDH3}-*CltLS1*-T_{CYC1}
B	P_{CCW12}-*tHMG1*-T_{TPSI1}
C	P_{CCW12}-*ERG20*^{F96WN127W}-T_{TPSI1}
D	P_{SSA1}-*ERG10*-T_{NAT1}-P_{RPL4A}-*ERG13*-T_{EFM1}-P_{RPL15A}-*tHMG1*-T_{EBS1}
E	P_{RPL4A}-*EfmvaS*-T_{EFM1}-P_{RPL15A}-EfmvaE-T_{EBS1}
F	P_{RPL8B}-*ERG12*-T_{NAT5}-P_{SSB1}-*ERG8*-T_{IDP1}-P_{RPL3}-*MVD1*-T_{PRM9}-P_{YEF3}-*IDI1*-T_{RPL15A}
G	P_{RPL8B}-*ERG12*-T_{NAT5}-P_{YEF3}-*IDI1*-T_{RPL15A}
A*	P_{TDH3}-*ERG20*^{F96WN127W}-Linker-*CltLS1*-T_{CYC1}
H	P_{SSB1}-*ERG8*-T_{IDP1}

the Results section.

2.7. Extraction and gas chromatography-mass spectrometry (GC-MS) quantification of limonene

For limonene detection, the dodecane samples were diluted in *n*-hexane (Thermo Scientific, 160780025) to prevent the quantification of the dodecane peak. Then, the mixture (1 μL) was analyzed by GC-MS using an Agilent System 6890 gas chromatograph coupled to an Agilent 5975 quadrupole mass selective detector (EI) (Agilent Technologies, Santa Clara, CA), equipped with an HP-5 (30 m × 0.25 mm, 0.25 μm film thickness) GC column. The GC oven temperature program was as follows: 100 °C for 1 min, a ramp of 0.5 °C/min to 102 °C, and then a rise to 280 °C in 5 min. The split ratio was 20:1. Helium was used as the carrier gas. The injector was kept at 280 °C, and the ion source temperature was 300 °C. Under the single ion monitoring (SIM) mode, the characteristic ions mass to charge ratio (*m/z*) named 68, 93, 121, and 136 were extracted from the GC−MS data for the standard quantification of limonene.

2.8. Extraction and liquid chromatography-mass spectrometry (LC-MS) analysis of metabolites

Single colonies were inoculated into YPD 2 % medium and cultivated overnight at 30 °C, 250 rpm. Subsequently, the seed culture was transferred into 10 mL of YPD 2 % medium with an initial OD600 of 0.2. After 24 h, 10^7 cells were transferred into 1.5 mL microcentrifuge tubes. Tubes were centrifuged at 1,500×*g* for 5 min, then the supernatant was carefully removed. The cell pellets were washed with 1 mL of ice-cold (4 °C) NaCl solution (150 mM) and centrifuged again at 1,500×*g* for 5 min. Then the washing solution was removed as thoroughly as possible. Subsequently, 300 μL of an 80 % [vol/vol] methanol solution (pre-cooled to −80 °C) was added, and the tubes were vortexed several times to ensure the pellet was fully dissolved. The samples were stored overnight at −80 °C. The following day, samples were centrifuged at 20,000×*g* for 15 min at 4 °C, and then the supernatant was transferred to new 1.5 mL microcentrifuge tubes for analysis.

Each sample (10 μL) was loaded into a Dionex UltiMate 3000 LC System (Thermo Scientific, Bremen, Germany) equipped with a C-18 column (Acquity UPLC HSS T3, 1.8 μm; 2.1 × 150 mm, Waters) and coupled to a Q Exactive Orbitrap mass spectrometer (Thermo Scientific) operating in negative ion mode. The separation was achieved using a step gradient with solvent A (10 mM TBA (Tetrabutylammonium) and 15 mM acetic acid) and solvent B (100 % methanol). The gradient started with 5 % solvent B and 95 % solvent A, held at 5 % B until 2 min post-injection, then transitioned linearly to 37 % B by 7 min, and to 41 % B by 14 min. From 14 to 26 min, the gradient increased to 95 % B, where it remained for 4 min, before returning to 5 % B at 30 min. Chromatography concluded at 40 min. The flow rate was constant at 0.25 mL/min, with the column maintained at 40 °C. The mass spectrometer operated in full scan mode (*m/z* range: 70–1050) with a spray voltage of 4.80 kV, capillary temperature of 300 °C, sheath gas at 40.0 L/min, and auxiliary gas at 10.0 L/min. The AGC target was set at 3.0×10^6, with a resolution of 140,000 and a maximum injection time of 512 ms. Data collection was performed using Xcalibur software (Thermo Scientific), and data analysis involved peak area integration using El-Maven (Polly - Elucidata).

2.9. Data analysis and statistics

To analyze statistical differences in the yeast niches in terms of limonene tolerance and lipid content, data from both screening processes were analyzed using Welch's ANOVA, and the Games-Howell post-hoc test (Origin, 2025 Pro). To do the phylogenetic analysis, amino acid sequences were aligned by Clustal Omega (Madeira et al., 2024), and a neighbor-joining tree was built in MEGA11. Whole-genome sequence data of strains were analyzed using QIAGEN CLC Main Workbench, and sequence alignment and visualization were performed in SnapGene. The phenotypic effect of an amino acid substitution was predicted by SIFT (https://sift.bii.a-star.edu.sg/www/SIFT_seq_submit2.html). The statistical significance of differences among selected and engineered limonene-producing strains and the type strain was assessed using a two-sided Student's t-test. To standardize and compare metabolite values across different distributions, Z-score normalization was used on metabolites data in R 4.2.0 (pheatmap package, scale() function). To verify the reproducibility of experiments, experiments were performed using biological replicates. Detailed information on the respective number of experimental replicates can be found in the individual figure legends.

3. Results and discussion

3.1. Screening genetically diverse yeast strains for limonene tolerance and lipid content

It is not known whether the main limitation of limonene production is its toxicity or the lack of cellular precursors in the producer. Since genetic background is expected to play a significant role in both processes, we first screened different strains from four yeast species—*S. cerevisiae*, *Yarrowia lipolytica*, *Lipomyces starkeyi*, and *Rhodosporidium toruloides* for limonene tolerance—with 921, 17, 10, and 8 strains of each species, respectively. We found that the phenotypic diversity within *S. cerevisiae* far exceeds the interspecies diversity in limonene tolerance, with the best *S. cerevisiae* strains showing much higher tolerance compared to the other species (Fig. S1). Therefore, we subsequently screened the panel of 921 genetically diverse *S. cerevisiae* strains, originating from 12 different niches (Fig. 1A), for limonene tolerance and lipid content.

Limonene tolerance was initially tested by assessing yeast growth in the presence of 300 mM limonene. At this concentration, none of the type strains (CEN.PK2-1C, S288C, W303) and only 431 (46 %) of the other strains grew to an OD600 above 1.0 (Fig. 1B, Table S1). Notably, tolerance to limonene showed significant variability among strains from different niches (F-value = 427.27, p-value = 0, Welch's ANOVA, Fig. 1B, Table S8). In general, strains from Cocoa, Various, and Sourdough niches showed significantly higher limonene tolerance compared to type strains (Games-Howell post-hoc test, $\alpha = 0.05$). Next, the type strain CEN.PK2-1C and seven genetically diverse, limonene-tolerant strains were evaluated in more detail to assess their tolerance to different limonene concentrations (500 mM, 1000 mM, and 1500 mM) (Fig. 1C). At 1000 mM, only two strains (a Wine strain Y119, and a Bread strain Y243) grew, and no growth was observed for any of the strains at 1500 mM (Fig. 1C). The strong limonene tolerance of strain Y243 may be attributed to its thicker cell wall and larger cell size (Fig. S2), which could provide enhanced protection against the toxic effects of limonene by reducing membrane permeability or increasing cellular robustness.

In parallel, inherent lipid accumulation was evaluated using Nile Red staining in the 921 *S. cerevisiae* strains (Fig. 1D, Table S1). Since lipid droplets are energy storehouses of surplus metabolic energy and lipids, supplying cells with metabolic building blocks such as acetyl-CoA (Olzmann and Carvalho, 2019; Son et al., 2022; Wei et al., 2018; Welte and Gould, 2017), we reasoned that increased lipid body content in *S. cerevisiae* might indicate increased acetyl-CoA production, which is a precursor for limonene synthesis. Once again, significant variation was observed among the 12 families of yeast strains (F-value = 14.48, p-value = 3.23×10^{-13}, Welch's ANOVA, Fig. 1D, Table S9). Specifically, strains from the Wild isolates, Bread, and Wine clades showed significantly higher lipid content compared to type strains (CEN.PK2-1C, S288C, W303) (Games-Howell post-hoc test, $\alpha = 0.05$). Based on these results, 34 strains with the highest lipid content and the type strain CEN.PK2-1C were selected and used in a follow-up experiment to validate their lipid content, leading to the identification of two Ale beer strains,

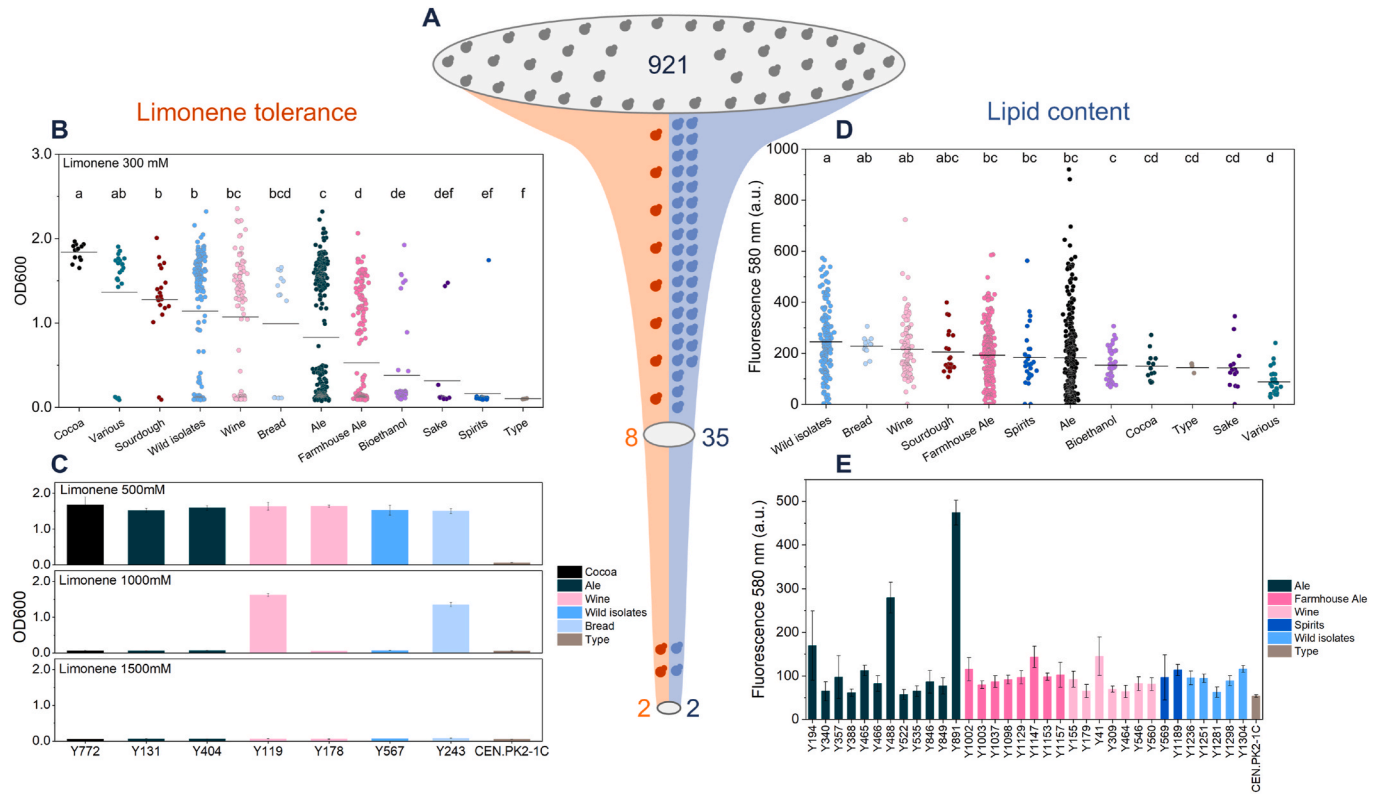

Fig. 1. Screening of 921 strains for limonene tolerance and lipid content variability. (A) Schematic view of the screening workflow. (B) Cell growth of 921 *S. cerevisiae* strains under 300 mM limonene in dodecane. The horizontal line in the middle of each niche indicates the mean. Letters a-f indicate groups of strains with significantly different limonene tolerance based on the Welch's ANOVA, Games-Howell post-hoc test, $\alpha = 0.05$. (C) Cell growth of seven selected industrial strains and the type strain CEN.PK2-1C in 500 mM, 1000 mM, and 1500 mM limonene. (D) Lipid fluorescence values of 921 strains. The horizontal line in the middle of each niche indicates the mean. Letters a-d indicate groups that show significantly different lipid content based on Welch's ANOVA, Games-Howell post-hoc test, $\alpha = 0.05$. (E) Lipid fluorescence values of 34 selected industrial strains and the type strain CEN.PK2-1C. All data in (C) and (E) are represented as mean ± SD of three biologically independent experiments. Twelve colors are used to indicate the niches of the strains. (For interpretation of the references to color in this figure legend, the reader is referred to the Web version of this article.)

Y891 and Y488, with the highest inherent lipid content (Fig. 1E).

Limonene tolerance did not correlate with lipid content (R-Square = 0.01206, p-value = 8.76833×10^{-4}, Fig. S3), suggesting that the strains may mitigate limonene toxicity by upregulating antioxidant enzymes and enhancing antioxidant levels (Brennan et al., 2013; Liu et al., 2013), independent of lipid accumulation (Graef, 2018). We compared lipid fluorescence values across 34 high-lipid-content strains, 7 strong-limonene-tolerant strains, and CEN.PK2-1C (Fig. S4), and the result showed that lipid content in these seven strong limonene tolerant strains are much lower than 34 lipid strains. Furthermore, industrial *S. cerevisiae* strains adapted to harsh fermentation environments have evolved to withstand several stress factors associated with industrial practices, including hydrostatic pressure, vigorous mixing and pumping, high sugar, ethanol, and/or CO_2 concentrations. Such domesticated industrial strains may therefore be particularly suited for implementation in full-scale industrial precision fermentation. Together, based on limonene tolerance and lipid content as key indicators, five chassis strains were selected for further genetic engineering: a Wine strain (Y119), a Bread strain (Y243), two Ale beer strains (Y891 and Y488), and the type strain CEN.PK2-1C as a control.

3.2. Characterization of different limonene synthases

Research has indicated that the poor monoterpene titers currently achieved are due to the suboptimal performance of monoterpene synthases (Su et al., 2024). Therefore, before engineering the selected chassis strains, we tested the performance of 16 limonene synthase genes (*LSs*) from 13 distinct plant species (Fig. 2A, Tables S4 and S5) in two strain backgrounds: the Bread strain Y243, which demonstrated good limonene tolerance and genetic engineering potential, and the CEN.PK2-1C type strain. Seven of those *LSs* had not been previously tested in yeast (Fig. 2A–Table S4 and S5) (Cheng et al., 2019). As the introduction of *LSs* alone led to low limonene titers (Fig. 2B), a mutated version of *ERG20* (*ERG20*$^{F96W-N127W}$) (Ignea et al., 2014) was also inserted before introducing the *LSs* into both strains. This is to enhance the supply of geranyl pyrophosphate (GPP), the direct limonene precursor.

Seven *LSs* resulted in detectable limonene production in CEN.PK2-1C, with *CltLS1* yielding the highest titer. Eight *LSs* yielded detectable limonene production in Y243, with *CltLS1* again exhibiting the highest titer. In both strains, *CltLS1*, *CstLS*, and *CltLS2* were consistently the best three variants. However, there were significant differences in limonene titers between CEN.PK2-1C and Y243 when expressing the same synthase (Fig. 2B). For the seven synthases that catalyzed limonene production in both strains, Y243 consistently achieved much higher titers, with at least a 6.9-fold increase compared to CEN.PK2-1C. Notably, when *ArtLS* was expressed, the limonene titer in Y243 was 23.7 times that of CEN.PK2-1C, underscoring the importance of chassis strain selection. Four of the newly tested synthases (*CatLS*, *SdtLS*, *PctLS*, and *SttLS*) successfully produced detectable limonene in Y243, thereby expanding the diversity of functional *LSs* for yeast. For systematic mining and evaluation of new terpene synthases, a high-yield terpene chassis is essential for efficient product production (Cheng et al., 2024). Although CEN.PK strains are commonly used as chassis for this purpose (Chen et al., 2021; Huang et al., 2023), strain Y243 presents a promising alternative as a high-yield chassis for efficient terpene product mining.

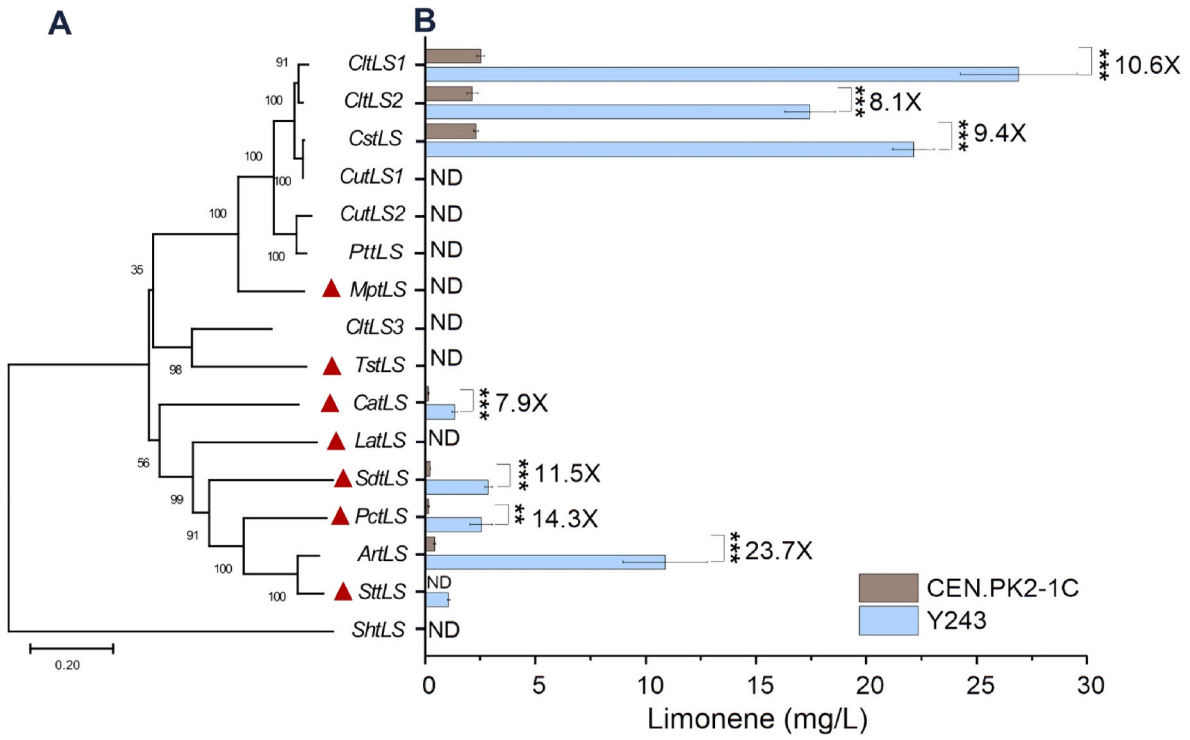

Fig. 2. Identification of high-efficiency limonene synthases. (A) Phylogenetic analysis of 16 tested limonene synthase genes (*LSs*) by using the neighbor-joining method. Numbers at each branch point indicate bootstrap values. Red triangles indicate *LSs* not previously reported for function in yeast. Alignment of amino acid sequences is shown in Fig. S5, and full plant species names are listed in Table S4. (B) Biosynthesis of limonene from 16 different *LSs* in CEN.PK2-1C and Y243. All data are represented as mean ± SD of three biologically independent experiments. ND indicates that no limonene could be detected in any of the three replicates. The numbers above bars are the fold changes between these 2 bars from low to high. Statistical significance was tested using the two-sided Student's t-test; **p < 0.01, ***p < 0.001. (For interpretation of the references to color in this figure legend, the reader is referred to the Web version of this article.)

Notably, the observed differences in activity may also reflect variations in protein expression levels across different strain backgrounds, rather than solely inherent differences in enzymatic activity. Moreover, we expressed the engineered limonene synthase *HCinS*^{N135H} (Su et al., 2024) in both Y243 and CEN.PK2-1C, and the result showed that *CltLS1* outperform *HCinS*^{N135H} under the strong promoter (P_{TDH3}) in both backgrounds (Fig. S6). Despite this variability, *CltLS1* was identified as the most effective synthase and was selected as the synthase to introduce in five selected chassis strains (a Wine strain Y119, a Bread strain Y243, two Ale beer strains Y891 and Y488, and the type strain CEN.PK2-1C).

3.3. Engineering limonene production in five selected chassis strains

To evaluate limonene production potential in the four identified chassis strains (Y119, Y243, Y891, and Y488), and the type strain CEN.PK2-1C (Table 2), we initially engineered these strains by targeting three key genes (shown in Fig. 3A). The selected limonene synthase gene from *Citrus limon* (*CltLS1*, indicated with a superscript "A" in the strain name). Next, a truncated version of the *HMGR* gene was overexpressed (*tHMG1*, indicated with superscript "B" in the strain name) to enhance the MVA pathway (Paramasivan and Mutturi, 2017). Finally, a mutant *ERG20* (*ERG20*$^{F96W-N127W}$, indicated with superscript "C" in the strain name) was introduced to improve GPP supply (Ignea et al., 2014).

Table 2
Five strains were selected from screening for genetic engineering.

Strain	Niche	Screening assay
CEN.PK2-1C	Type strain	–
Y488	Ale Beer	High lipid content
Y891	Ale Beer	High lipid content
Y119	Wine	Strong limonene tolerance
Y243	Bread	Strong limonene tolerance

No limonene was detected in the wild-type strains lacking a functional limonene synthase (Fig. S7). However, after introducing *CltLS1*, all strains produced limonene, although titers were generally low. Limonene titers ranged from 0.5 mg/L in CEN.PK2-1C^{A} to 3.7 mg/L in Y243^{A}. Compared to CEN.PK2-1C^{A}, limonene titers in all four industrial strains were 3.8-fold, 3.9-fold, 3.7-fold, and 7.1-fold higher, respectively (Fig. 3B). These differences may at least be partly caused by the higher copies numbers of *CltLS1* gene integrated into the chromosomes of the polyploid strains. While the haploid CEN.PK2-1C^{A} only contains one copy of a construct, the diploid Y119^{A} contains two copies, and the tetraploid Y243^{A}, Y488^{A} and Y891^{A} contain four copies (Fig. S8, Fig. S9). Importantly, strains with the same ploidy do not always display the same limonene titers, indicating effects other than copy number effects. Notably, Y488^{A}, Y891^{A}, and Y243^{A} produced significantly higher amounts of limonene than CEN.PK2-1C^{A} (Fig. 3B). In this step, we also created S288C^{A}; however, since it produced lower limonene levels than CEN.PK2-1C^{A} (Fig. S10), further engineering of S288C was not pursued. Next, we introduced *tHMG1* to the strains with *CltLS1*, but no statistically significant differences were observed when comparing each industrial strain to CEN.PK2-1 C^{AB} (Fig. 3B). This effect is likely due to the fact that the introduction of *tHMG1* did not consistently increase limonene titers across all strains (Fig. S7). As expected, *tHMG1* led to a 2.8-fold increase in CEN.PK2-1C^{AB} (Fig. S7), but only a marginal 0.2-fold increase in strains Y488^{AB}, Y891^{AB}, and Y119^{AB} (Fig. S7). In contrast, strain Y243^{AB} showed a 30 % decrease after the introduction of *tHMG1* (Fig. S7). While *HMGR* is commonly identified as a rate-limiting gene in the MVA pathway in CEN.PK strains (Cao et al., 2023; Jiang et al., 2021), this may not hold true for strain Y243. We then introduced *ERG20*$^{F96W-N127W}$ to the strains with *CltLS1*, which significantly boosted limonene production across all strains, ranging from 2.5 mg/L in CEN.PK2-1C^{AC} to 26.9 mg/L in Y243^{AC} (Fig. 3B, Fig. S7). Limonene titers in

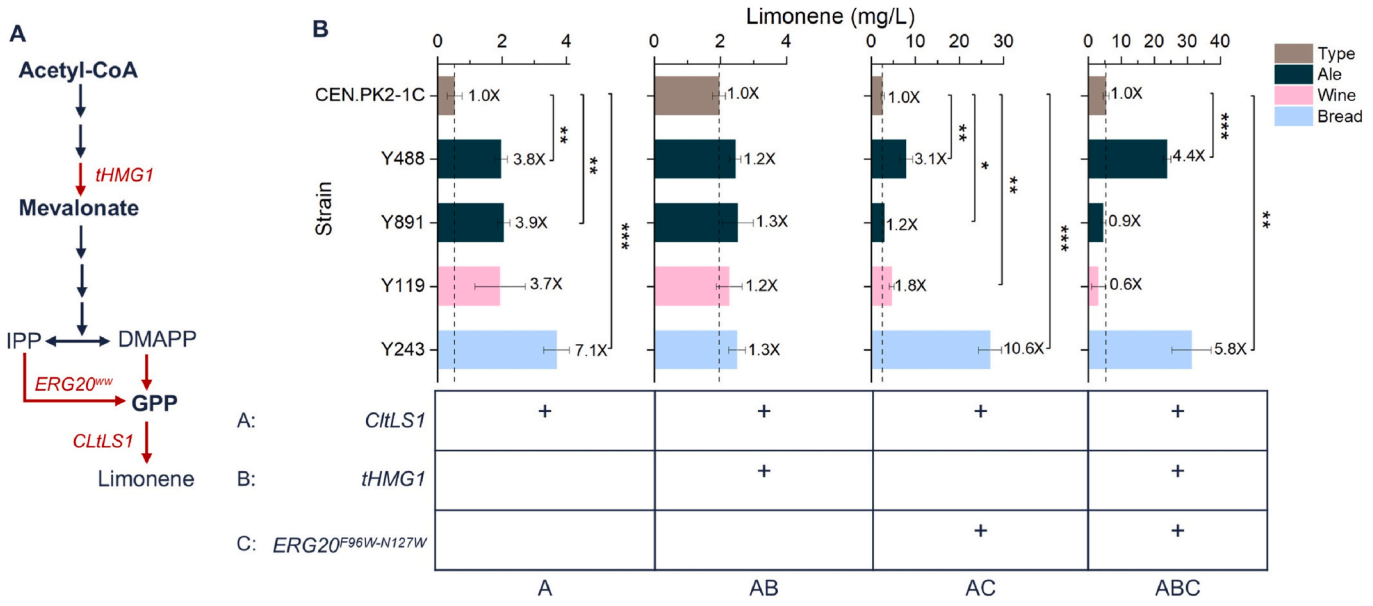

Fig. 3. Genetic engineering of five strains to establish limonene biosynthesis. (A) Schematic representation of the genetic engineering strategies to establish limonene biosynthesis. *tHMGR*, truncated HMG-CoA reductase. *ERG20^{ww}*, farnesyl pyrophosphate synthetase with two mutations. *CltLS1*, limonene synthase from *Citrus limon*. IPP, isopentenyl diphosphate. DMAPP, dimethylallyl diphosphate. GPP, geranyl diphosphate. (B) Limonene titers in five engineered strains. All data are represented as mean ± SD of three biologically independent experiments. The numbers above bars are the fold changes compared to the first bar in each plot. Statistical significance was tested using the two-sided Student's t-test; **p < 0.01, ***p < 0.001; and those with p > 0.05 were not labeled.

Y488^{AC}, Y891^{AC}, Y119^{AC}, and Y243^{AC} were significantly higher than the titer in CEN.PK2-1C^{AC}, respectively. (Fig. 3B). Notably, the limonene titer in strain Y243^{AC} rose dramatically to 26.9 mg/L from 3.7 mg/L (a 6.3-fold increase), suggesting that GPP availability is a particularly strong bottleneck in this strain. Finally, when introducing both *tHMG1* and *ERG20$^{F96W-N127W}$* to the strain with *CltLS1*, limonene production increased in all strains as well though to different extents (Fig. S7). Strain Y243^{ABC} was still the highest producer, achieving a titer of 31.2 mg/L, while the limonene titer in Y488^{ABC} increased to 23.9 mg/L, both significantly outperforming CEN.PK2-1C^{ABC} (5.4 mg/L) (Fig. 3B).

Overall, all selected strains showed between 3.7 to 7.1-fold higher limonene production than the type strain CEN.PK2-1C after engineering. This observation already highlights the importance of testing different backgrounds for microbial cell factory engineering approaches. Since Y243^{ABC} and Y488^{ABC} showed the most promising limonene titers, these strains (together with CEN.PK2-C^{ABC}) were selected for further engineering.

3.4. Modular metabolic engineering of the MVA pathway

To further boost limonene production and investigate how the chassis strains respond to different MVA engineering strategies, we systematically engineered the MVA pathway in the two selected chassis strains (Y488^{ABC} and Y243^{ABC}) and the type strain (CEN.PK2-1C^{ABC}) (Fig. 4A). Specifically, we overexpressed two different variants of the upper MVA module: (i) a native variant consisting of three genes (*ERG10*, *ERG13*, t*HMG1*; denoted as ScMVA_upper module and indicated with superscript "D" in the strain name) and (ii) a bacterial variant from *Enterococcus faecalis* comprising two genes (E: *EfmvaS*, *EfmvaE*; denoted as EfMVA_upper module and indicated with superscript "E" in the strain name). In addition, we overexpressed the native lower MVA pathway starting from mevalonate to isopentenyl diphosphate (IPP) and dimethylallyl diphosphate (DMAPP), encoded by the genes *ERG12*, *ERG8*, *ERG19*, and *IDI1* (denoted as ScMVA_lower module and indicated with superscript "F" in the strain name) (Peng et al., 2017).

Overexpression of the upper MVA pathway modules (D: ScMVA_upper module or E: EfMVA_upper module) only benefited strain Y488$^{ABCD/E}$, leveraging limonene titers by approximately 2.5-fold to approximately 70 mg/L (Fig. 4B). This was nearly 14-fold higher than CEN.PK2-1C$^{ABCD/E}$ (Fig. S11). These results suggest that the genes in the upper MVA module may be limiting steps in Y488^{ABC}, but not in CEN.PK2-1C^{ABC} and Y243^{ABC}. In contrast, overexpression of the lower MVA pathway module (F: ScMVA_lower) had a more significant effect, with all strains showing an increase in titer (varying from 50 % increase in Y488^{ABCF} to 350 % in Y243^{ABCF}) (Fig. 4B). These results suggest that the genes in the lower module may be limiting steps in CEN.PK2-1C^{ABC} and Y243^{ABC}, but to a lesser extent in Y488^{ABC}. After overexpressing ScMVA_lower, the limonene titer in Y243^{ABCF} (141.6 mg/L) was 6.6-fold higher than that in CEN.PK2-1C^{ABCF} (21.5 mg/L)(Fig. S11).

Combined overexpression of the upper and lower modules of the MVA pathway resulted in the strongest increase across all strains (Fig. 4B). Limonene titers reached 75.2 mg/L and 66.4 mg/L in CEN.PK2-1C^{ABCDF} and CEN.PK2-1C^{ABCEF}, 172.8 mg/L and 185.4 mg/L in Y243^{ABCDF} and Y243^{ABCEF}, and 152.8 mg/L and 197.8 mg/L in Y488^{ABCDF} and Y488^{ABCEF} (Fig. 4B). After the complete MVA pathway overexpression, limonene titers of the two selected industrial strains were still at least 2-fold higher than those in CEN.PK2-1C (Fig. 4B, Fig. S11). Strain Y488^{ABC} showed a modest improvement with the upper and lower pathway modifications individually, but the combination of both modules resulted in the highest performance, achieving nearly 200 mg/L. This synergistic effect suggests multiple bottlenecks in the MVA pathway in strain Y488^{ABC}. Replacing one module improves its performance, but the full pathway enhances it more significantly.

Notably, limonene titers in all strains with ScMVA_upper module (strain^{ABCD}) were significantly higher than those with EfMVA_upper module (strain^{ABCE}). However, when the ScMVA_lower module was added to strains, no significant difference was observed between strain^{ABCDF} and strain^{ABCEF} (Fig. 4B). These most likely suggest that the lower MVA pathway module remains the rate-limiting step so that differences caused by overexpressing the upper module (ScMVA_upper and EfMVA_upper) are obscured. Moreover, owing to the good performance of the EfMVA_upper module in *S. cerevisiae* (Dusseaux et al., 2020; Jiang et al., 2017), we decided to further enhance the flux of the lower MVA pathway module in strains^{ABCEF}.

We targeted two key genes in the lower MVA pathway module. Firstly, *ERG12*, which channels mevalonate into the pathway

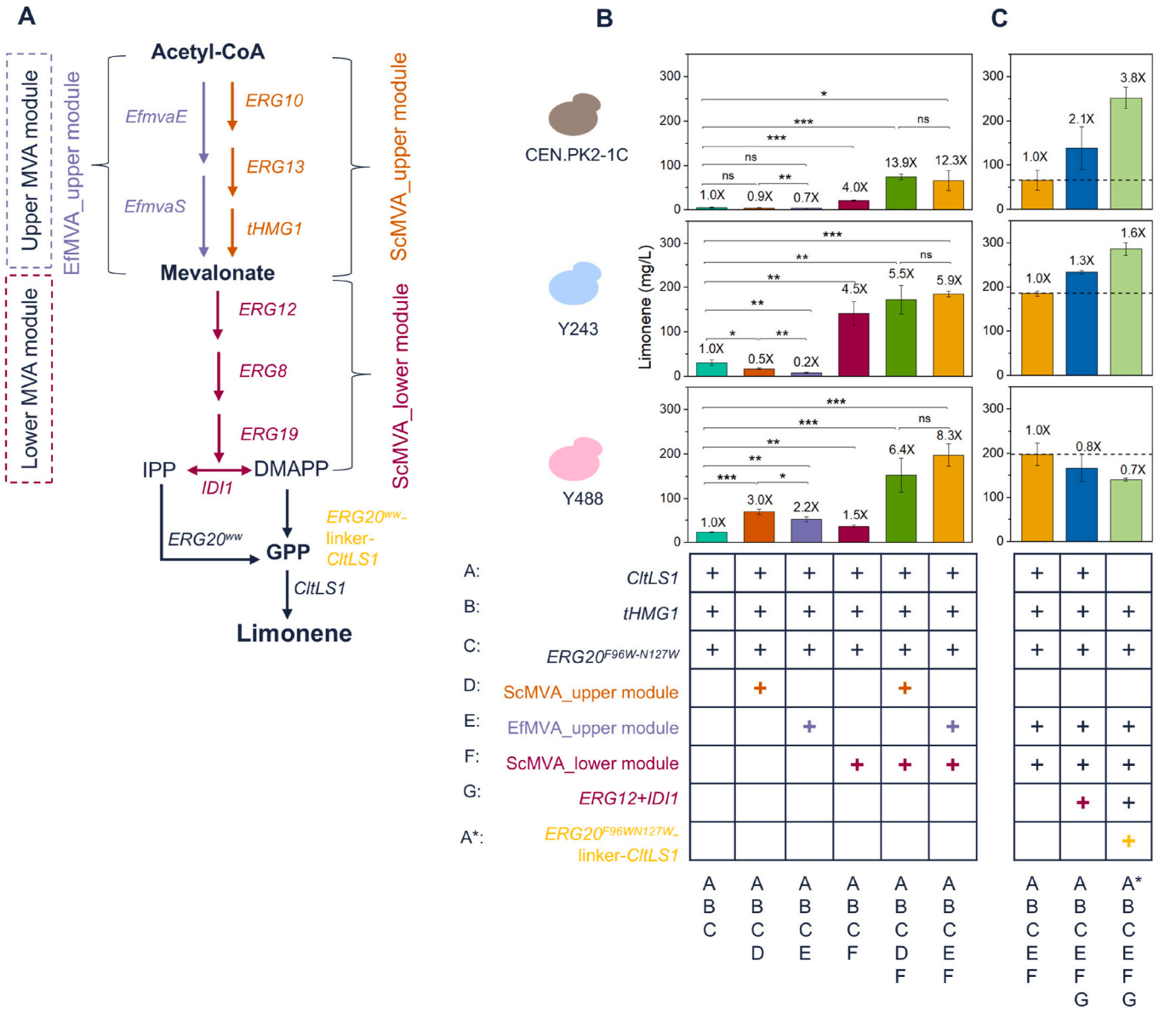

Fig. 4. Modular engineering of the mevalonate (MVA) pathway for limonene biosynthesis in three strains. (A) Schematic view of the modular engineering strategies for limonene biosynthesis. The MVA pathway was divided into two modules: the upper-pathway module (shown in orange and purple) and the lower-pathway module (shown in pink). *ERG10*, acetoacetyl-coenzyme A thiolase. *ERG13*, 3-hydroxy-3-methylglutary-CoA (HMG-CoA) synthase. *tHMGR*, truncated HMG-CoA reductase. *EfMvaE* and *EfMvaS* are from *Enterococcus faecalis*; *EfmvaE*, acetoacetyl-coenzyme A thiolase, and HMG-CoA reductase; *EfMvaS*, HMG-CoA synthase. *ERG12*, mevalonate kinase. *ERG8*, phosphomevalonate kinase. *ERG19*, mevalonate pyrophosphate decarboxylase. *IDI*, IPP: DMAPP isomerase. *ERG20^{ww}*, farnesyl pyrophosphate synthetase with two mutations. *CltLS1*, limonene synthase from *Citrus limon*. *ERG20^{ww}-linker- CltLS1*, a fusion that these two genes was linked by an AG4TGGA linker. IPP, isopentenyl diphosphate. DMAPP, dimethylallyl diphosphate. GPP, geranyl diphosphate. (B) Limonene titers changed after each module of the MVA pathway was overexpressed in three strains individually and in combination. (C) Two genes (*ERG12*, *IDI1*) in MVA_lower were further overexpressed and a fusion of *CltLS1* and *ERG20^{WW}* was expressed in three strain^{ABCEF} backgrounds. Letters A-G indicate gene constructs (provided in Table 1) used for labeling engineered strains. The numbers above bars are the fold changes compared to the first bar in each plot. All data are represented as mean ± SD of three biologically independent experiments. Statistical significance was tested using the two-sided Student's t-test; *p < 0.05, **p < 0.01, ***p < 0.001, and ns p > 0.05. (For interpretation of the references to color in this figure legend, the reader is referred to the Web version of this article.)

(Mukherjee et al., 2022), and secondly, *IDI1*, which plays a critical role in maintaining the balance between IPP and DMAPP (Jiang et al., 2017), resulting in strain^{ABCEFG} (where the letter G refers to the combined overexpression of *ERG12* and *IDI1*) (Fig. 4C). Additionally, to increase synthase accumulation, *CltLS1* was replaced with a translational fusion between *CltLS1* and *ERG20^{ww}* via an AG4TGGA linker (referred to as A*: *ERG20^{ww}*-linker-*CltLS1*) (Cheah et al., 2023), resulting in strain^{A*BCEFG} (Fig. 4C). After these two additional engineering steps, limonene titers further increased compared to strain^{ABCEF}, with a maximum of 1.6-fold in Y243^{A*BCEFG} and 3.8-fold in CEN.PK2-1C^{A*BCEFG} (Fig. 4C). Conversely, the limonene titers in strain Y488 decreased slightly after the two additional engineering steps (Y488^{ABCEFG} and Y488^{A*BCEFG} exhibited 0.8-fold and 0.7-fold limonene reduction compared to Y488^{ABCEF}). Once more, these results suggest that there are multiple bottlenecks in the MVA pathway in strain Y488^{ABC} and the upper MVA module may be more limiting than the lower one. Additionally, Y488^{ABCEF} may have reached its limonene tolerance limit, as it was selected for high lipid content rather than strong limonene tolerance.

In summary, the contribution of each engineering step to limonene production was highly strain-dependent, emphasizing the need for

tailored strategies for each chassis strain. Strategies optimized for the type strain CEN.PK2-1C did not perfectly translate to the industrial strains, indicating that there does not appear to be a 'one-engineering-strategy-fits-all' approach for creating efficient microbial cell factories.

3.5. Metabolite profiling reveals strain-specific bottlenecks in the MVA pathway

To gain deeper insights into the differences between the type strain CEN.PK2-1C and the chassis strain Y243 that produced the highest titers as mentioned above, we performed a metabolomics assay (LC/MS) to quantify ten main intermediates of the isoprenoid pathway (Fig. 5, Table S10). This analysis was conducted for the wild type (WT) and four engineered variants (strain^{ABCDF}, strain^{ABCEF}, strain^{ABCEFG}, strain^{A*BCEFG}) of both CEN.PK2-1C and Y243.

Comparison of the CEN.PK2-1C^{WT} and Y243^{WT} strains (Fig. 5, Fig. S12B) in the upper MVA pathway showed that the MVA flux is indeed different between CEN.PK2-1C^{WT} and Y243^{WT} (Fig. 5, Fig. S12B). HMG-CoA level was higher in CEN.PK2-1C^{WT}, while the MVA level was higher in Y243^{WT}. This suggests that the flux between the two compounds is naturally slower in CEN.PK2, in line with the greater impact *tHMG1* expression had on limonene production in CEN.PK2-1C^{AB} (Fig. 3B). And then, in the lower MVA pathway, more GPP (2.4-fold) and FPP (18.6-fold) accumulated in Y243^{WT}, indicating that Y243^{WT} shows stronger flux towards both GPP and FPP (Fig. 5, Fig. S12B). Amino acid sequence alignment of eight key isoprenoid pathway enzymes (Erg10, Erg13, Hmg1, Erg12, Erg8, Erg19, Idi1, and Erg20) of the high-limonene-producing strain Y243 and reference strain CEN.PK113-7D (a prototrophic CEN.PK2-1C derivative) revealed amino acid polymorphisms in three lower MVA pathway enzymes (Erg12, Erg8, Erg19; Table S11). These mutations might contribute to the observed accumulation of downstream metabolites (Fig. 5, Fig. S12B) and may therefore be interesting targets for improving terpene production in other strains.

When it came to the comparison of the CEN.PK2-1C$^{ABCD/EF}$ and Y243$^{ABCD/EF}$, after overexpressing the complete MVA pathway, the metabolite profiles of both strains changed dramatically compared to the respective WT strains (Fig. 5B and C, Fig. S12C). First, HMG-CoA was nearly undetectable in engineered strains, suggesting that the overexpression of *tHMG1* and *EfMvaE* drives the efficient conversion of HMG-CoA to MVA. Notably, the MVA levels in CEN.PK2-1C/Y243^{ABCEF} were significantly higher than in CEN.PK2-1C/Y243^{ABCDF} (Fig. 5B and C, Fig. S12C), suggesting that the EfMVA_upper module converted acetyl-CoA more efficiently into MVA, and this finding aligns with several previous studies (Dusseaux et al., 2020; Luo et al., 2019; Ma et al., 2023). However, the higher level of MVA caused by overexpressing EfMVA_upper was not efficiently converted into the final product limonene (Fig. 4B), because no significant differences was observed in limonene titers between CEN.PK2-1C^{ABCDF} and CEN.PK2-1C^{ABCDEF}, Y243^{ABCDF} and Y243^{ABCEF} (Fig. 4B).

Next, in strain CEN.PK2-1C^{ABCEFG} and Y243^{ABCEFG} with additional overexpression of *ERG12* and *IDI1*, we observed decreased levels of MVA and IPP/DMAPP, accompanied by improvements in limonene titers (Fig. 5, Fig. S12D). This implies that these two genes in the lower MVA pathway channeled MVA into limonene. Lastly, when *CltLS1* was replaced by a fusion (*ERG20^{WW}*-linker-*CltLS1*) to create CEN.PK2-1C^{A*BCEFG} and Y243^{A*BCEFG}, limonene titers significantly increased in both strains as expected (Fig. 4C). However, metabolite levels varied between the two similarly engineered strains. In CEN.PK2-1C^{A*BCEFG}, acetyl-CoA, MVA5P, MVA5PP, IPP/DMAPP, and GPP levels were increased compared to CEN.PK2-1C^{ABCEFG}. In contrast, Y243^{A*BCEFG} showed decreased levels of acetyl-CoA and FPP and increased levels of MVA, MVA5PP, and GPP, the latter suggesting that the conversion of GPP into limonene remains a bottleneck. Lastly, MVA and MVA5P showed higher accumulation in Y243-derived strains, suggesting that Erg8 might be a rate-limiting enzyme in Y243^{A*BCEFG}(Fig. 5, Fig. S12D).

Overall, comparative metabolomics of ten key intermediates of the isoprenoid pathway revealed differences in the metabolite profile between Y243 and CEN.PK2-1C, both for the WT and engineered versions of these strains. Strain Y243 accumulated higher levels of MVA and MVA5P than CEN.PK2-1C, which likely contributed to its superior limonene production. In addition, genome analysis of Y243 shows that it is an allotetraploid strain. This genotype may also contribute to the strain's superior performance because hybrids often show heterosis for certain phenotypes (Gallone et al., 2016; Steensels et al., 2014b). Moreover, the tetraploid background also implies that all constructs are present in four copies, which may further contribute to the superior performance of Y243. Based on the hypothesis that intermediates accumulate prior to flux limitations, we adopted the concept of rate-limiting steps. Under this framework, the observed differences in metabolites and native metabolic fluxes might explain why engineering strategies need not be the same for strains harboring differences in their native metabolic flux balance.

3.6. Boosting limonene biosynthesis in CEN.PK2-1C^{A*BCEFG} and Y243^{A*BCEFG} using strain-specific engineering approaches

Guided by the differences in metabolite profiles in strain CEN.PK2-1C^{A*BCEFG} and Y243^{A*BCEFG}, we developed strain-specific engineering strategies in an attempt to further boost limonene biosynthesis in these two strains. For CEN.PK2-1C^{A*BCEFG}, the *ERG20^{WW}*-linker-*CltLS1* (A*) fusion was further overexpressed to divert more accumulated GPP to limonene. For Y243^{A*BCEFG}, we overexpressed *ERG8* (indicated by the letter H) to boost MVA5P conversion into MV5PP.

In strain CEN.PK2-1C^{A*BCEFG}, the introduction of a second copy of the *ERG20^{WW}*-linker-*CltLS1* fusion resulted in a 101 % increase in limonene titer, reaching 536 mg/L in CEN.PK2-1C$^{(A*2x)BCEFG}$ (Fig. 6A). On top of that, introducing a third copy of the *ERG20^{WW}*-linker-*CltLS1* fusion resulted in an additional 20 % increase in limonene titer, yielding 605 mg/L in CEN.PK2-1C$^{(A*3x)BCEFG}$ (Fig. 6A). These results confirmed that the conversion of GPP into limonene constitutes a major bottleneck in strain CEN.PK2-1C^{A*BCEFG}.

In contrast, the introduction of *ERG8* into strain Y243^{A*BCEFG} did not result in a significant increase of limonene production as had been expected (Fig. 6B). We hypothesized that while overexpression of *ERG8* may have addressed MVA5P accumulation, the final conversion to limonene was still limited (as seen for the CEN.PK2-1C strains). Therefore, we introduced an extra *ERG20^{WW}*-linker-*CltLS1* fusion to drive the flux, and this resulted in a 149 % increase in limonene titer, reaching 583 mg/L in Y243$^{(A*2x)BCEFGH}$ (Fig. 6B). This indicates that overexpressing the synthase genes at the end of the pathway pulls the fluxes from the upper pathway. Furthermore, introducing a third copy of the *ERG20^{WW}*-linker-*CltLS1* fusion resulted in a further 45 % increase in limonene titer, reaching 844 mg/L in Y243$^{(A*3x)BCEFGH}$ (Fig. 6B). This highlights the importance of balancing *LS* and lower MVA pathway expression to maximize limonene titers.

Notably, if the strain-specific engineering strategies were used on the other strain (this way generating CEN.PK2-1C/Y243$^{(A*3x)BCEFG}$ and CEN.PK2-1C/Y243$^{(A*3x)BCEFGH}$), we observed only a limited increase (12 %) in limonene production in both CEN.PK2-1C/Y243$^{(A*3x)BCEFGH}$ (CEN.PK2-1C$^{(A*3x)BCEFGH}$ vs. CEN.PK2-1C$^{(A*3x)BCEFG}$ and Y243$^{(A*3x)BCEFGH}$ vs. Y243$^{(A*3x)BCEFG}$ (Fig. S13). This finding again highlights the strain-specificity of optimal engineering strategies and the importance of metabolomics-aided strain design. Ultimately, the limonene titer achieved in strain Y243$^{(A*3x)BCEFGH}$ is 24 % higher (statistically significant, p-value = 0.02, two-sided Student's t-test) than the titer achieved in CEN.PK2-1C$^{(A*3x)BCEFGH}$ (Fig. S13). Limonene has been produced in various microorganisms, with *S. cerevisiae* achieving the highest reported titers, primarily in CEN.PK strains. These titers, obtained using inducible promoters (P_{GAL1} or P_{GAL10}) and optimized fed-batch fermentations, exceeded the highest titer in our study (844 mg/L in Y243). However, our results show that Y243 outperforms CEN.PK2-1C for

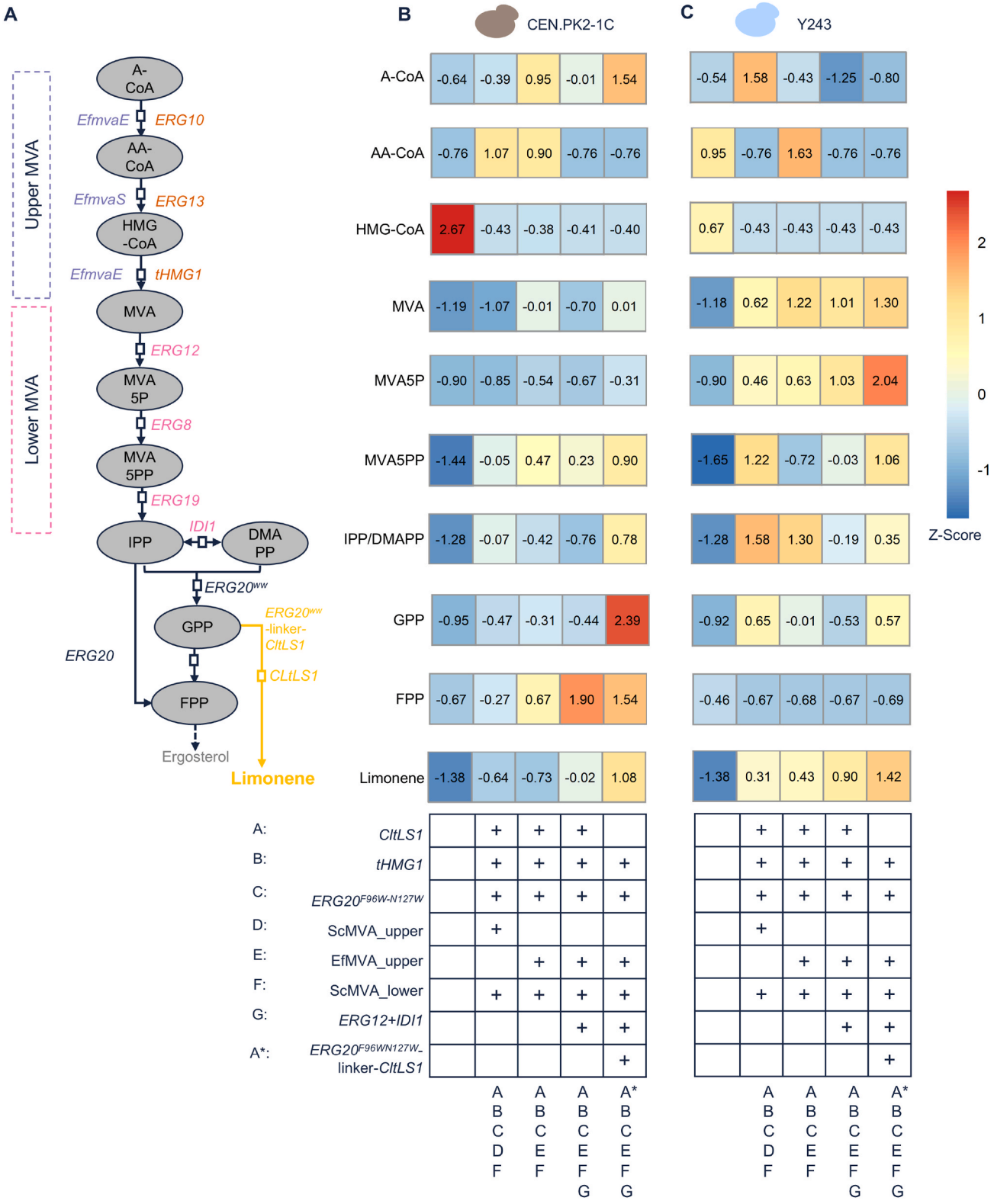

Fig. 5. Comparison of the 10 main metabolites of the isoprenoid pathway in wild types and engineered CEN.PK2-1C and Y243 strains. (A) Metabolite flow of the isoprenoids pathway; Metabolites abbreviations: A-CoA, acetyl-CoA; AA-CoA, acetoacetyl-CoA; HMG-CoA, 3-hydroxy-3-methyl-glutaryl-CoA; MVA, mevalonate; MVA5P, mevalonate 5-phosphate; MVA5PP, mevalonatepyrophosphate; IPP, isopentenyl diphosphate. DMAPP, dimethylallyl diphosphate. GPP, geranyl diphosphate; FPP, farnesyl pyrophosphate. All compounds were detected with high selectivity, except for IPP and DMAPP, which cannot be separated by the chromatographic method (Castano-Cerezo et al., 2019). (B) Metabolite changes in strain CEN.PK2-1C^{WT}, CEN.PK2-1C^{ABCDF}, CEN.PK2-1C^{ABCEF}, CEN.PK2-1C^{ABCEFG} and CEN.PK2-1C^{A*BCEFG}. (C) Metabolite changes in strain Y243^{WT}, Y243^{ABCDF}, Y243^{ABCEF}, Y243^{ABCEFG} and Y243^{A*BCEFG}. Numbers on plots (B) and (C) represent Z-score values to show how far a data point is from the mean of a dataset, and data was normalized per metabolite. $Z > \pm 1.96$ are considered statistically significant changes.

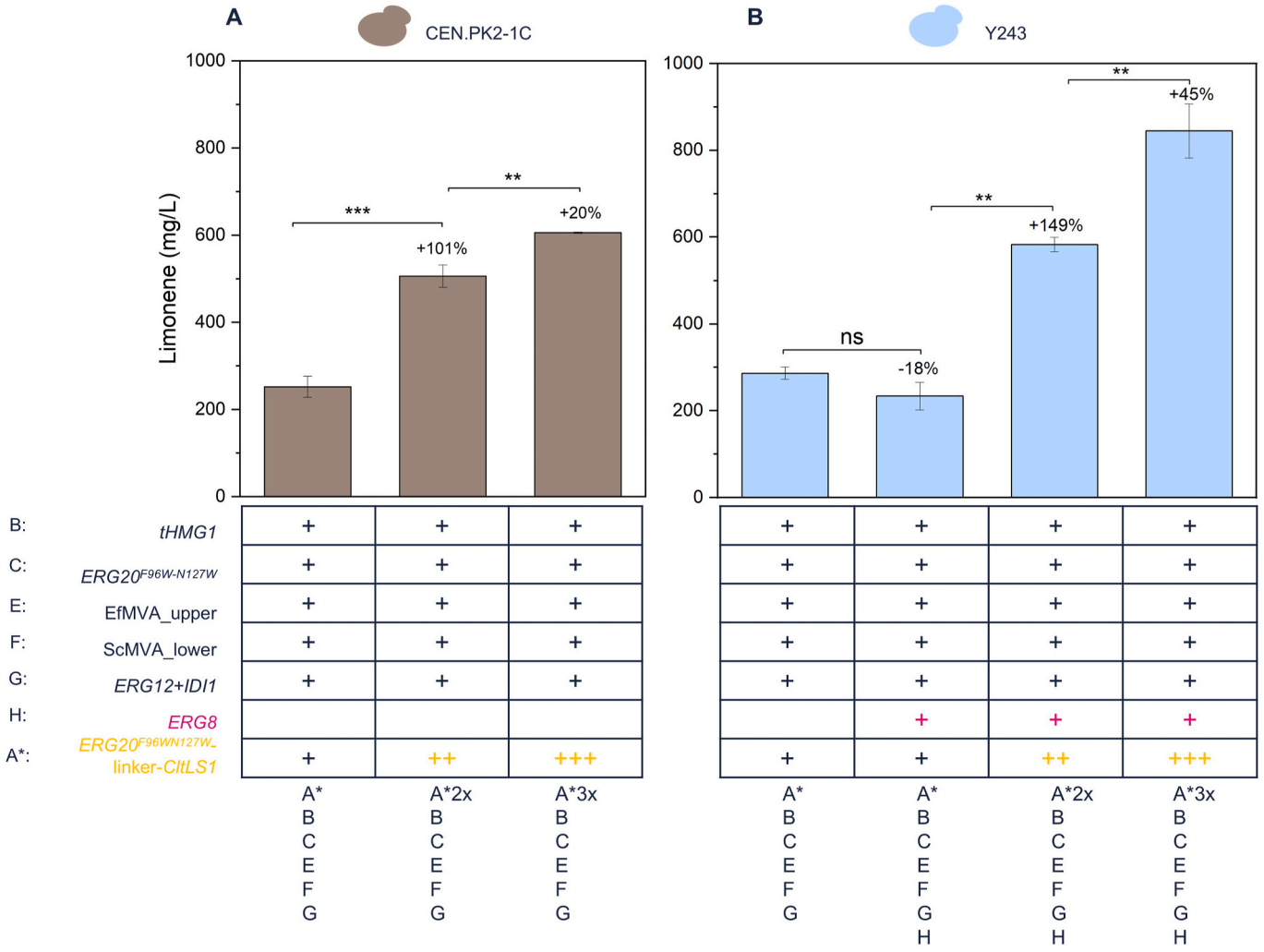

Fig. 6. Establishing efficient limonene biosynthesis in strain CEN.PK2-1C and Y243 using a strain-specific engineering approach. (A) Limonene titers for various engineered CEN.PK2-1C strains. (B) Limonene titers for various engineered Y243 strains. Letters A-H indicate gene constructs (provided in Table 1) used for labeling engineered strains. All data are represented as mean ± SD of three biologically independent experiments. The numbers above bars are the increase compared to the previous bar in each plot. Statistical significance was tested using the two-sided Student's t-test; *p < 0.05, **p < 0.01, ***p < 0.001, and ns p > 0.05.

limonene production under the conditions tested here, suggesting that Y243 may be able to surpass the reported titers upon further optimization of the fermentation conditions and gene expression levels. Our study also demonstrates that each strain requires a specific, tailored engineering strategy to reach its maximal potential. We hypothesize that Y243 titers can be further improved through the implementation and optimization of fed-batch cultures, AI-guided enzyme engineering, genome-scale metabolic models (GeMs)-guided pathway engineering, and optimized fermentation setups.

4. Conclusions

Engineering more efficient microbial cell factories to produce chemicals, fuels, and pharmaceuticals is crucial for realizing the full potential of precision fermentation. Various strategies have been developed to address these issues, but most typically focus on only one or a handful of strains, often the commonly used type strain CEN.PK2-1C.

In this study, we adopted the industrially relevant and cytotoxic monoterpene limonene as an outlet to assess whether and how chassis strains influence the optimal engineering strategy. Through massive screening, we identified two strains (Y119, Y243) with exceptional tolerance to limonene, and two strains (Y488, Y891) with high lipid content. Meanwhile, we identified four new limonene synthases (*CatLS*, *SdtLS*, *PctLS*, and *SttLS*) and proved that *CltLS1* is the most efficient one among them. These newly validated limonene synthases could be used as a starting point, e.g. rational engineering or random mutagenesis approaches, to develop improved variants. When the MVA pathway was systematically and parallelly engineered in the selected industrial strains, two of the selected strains showed approximately a 2-fold increase in titers compared to CEN.PK2-1C with the same genetic modifications. Ultimately, by using strain-specific engineering strategies, we achieved 844 mg/L in a new strain, which is 40 % higher than the optimal titer (605 mg/L) achieved in CEN.PK2-1C. Metabolite profiling indicated that Y243 accumulated higher levels of mevalonate than CEN.PK2-1C, which contributed to its enhanced production capability.

The selected industrial strains, especially strain Y243, exhibited significant advantages in both limonene tolerance and production. The strains described in this work could serve as chassis strains for the production of other monoterpenes. The comparative metabolomics approach not only identifies rate-limiting steps but also provides a framework for guiding strain engineering by targeting pathways with negative Z-scores across intermediates. This strategy highlights the potential to optimize metabolic flux toward the desired product. Furthermore, the data generated from intermediate constructs could serve as a training dataset for machine learning (ML) models, enabling ML-guided

engineering to design constructs that minimize Z-scores for all intermediates and enhance overall pathway efficiency.

Taken together, our findings underscore the importance of chassis selection through extensive screening, as well as the need for targeted metabolic engineering, which can vary significantly depending on the strain background.

CRediT authorship contribution statement

Yanmei Zhu: Writing – review & editing, Writing – original draft, Visualization, Validation, Software, Methodology, Investigation, Formal analysis, Data curation, Conceptualization. **Sasha Yogiswara:** Writing – review & editing, Visualization, Methodology, Investigation. **Anke Willekens:** Writing – review & editing, Validation, Methodology, Investigation, Data curation. **Agathe Gérardin:** Writing – review & editing, Visualization, Methodology, Investigation, Data curation. **Rob Lavigne:** Writing – review & editing, Supervision, Methodology, Investigation, Conceptualization. **Alain Goossens:** Writing – review & editing, Visualization, Supervision, Methodology, Conceptualization. **Vitor B. Pinheiro:** Writing – review & editing, Supervision, Methodology, Investigation, Conceptualization. **Zongjie Dai:** Writing – review & editing, Supervision, Project administration, Methodology, Investigation, Funding acquisition, Conceptualization. **Kevin J. Verstrepen:** Writing – review & editing, Validation, Supervision, Resources, Project administration, Methodology, Investigation, Funding acquisition, Formal analysis, Conceptualization.

Declaration of generative AI and AI-assisted technologies in the writing process

During the preparation of this work the author(s) used ChatGPT in order to improve language and readability, with caution. After using this tool/service, the author(s) reviewed and edited the content as needed and take(s) full responsibility for the content of the publication.

Declaration of Competing Interest

The authors declare that they have no competing interests.

Acknowledgments

This work was supported by a CSC (China Scholarship Council) PhD fellowship (CSC No. 202008440364) to Yanmei Zhu; a PhD fellowship from FWO (1S22422N) to Sasha Yogiswara and an FWO Extra-European Bilateral Research Project (G0E8222N) to Kevin J. Verstrepen; a National Natural Science Foundation of China (32161133019) and Tianjin Synthetic Biotechnology Innovation Capacity Improvement Project (TSBICIP-IJCP-002) to Zongjie Dai. The Special Research Fund (iBOF/21/092) to Rob Lavigne, Vitor B. Pinheiro, and Kevin J. Verstrepen. The authors are grateful to Dr. Karin Voordeckers and Dr. Jan Steensels for reviewing and editing the manuscript. The authors thank Dr. Quinten Deparis for bioinformatics analysis. The authors thank Dr. Beatriz Herrera-Malaver for setting up the detection method on GC-MS, and the VIB Metabolomics Core for metabolites detection on LC-MS.

Appendix A. Supplementary data

Supplementary data to this article can be found online at https://doi.org/10.1016/j.ymben.2025.04.011.

Data availability

Data is included in the manuscript.

References

Anandakumar, P., Kamaraj, S., Vanitha, M.K., 2021. D-limonene: a multifunctional compound with potent therapeutic effects. J. Food Biochem. 45 (1), e13566. https://doi.org/10.1111/jfbc.13566.

Bernard, A., Cha, S., Shin, H., Lee, D., Hahn, J.S., 2024. Efficient production of (S)-limonene and geraniol in Saccharomyces cerevisiae through the utilization of an Erg20 mutant with enhanced GPP accumulation capability. Metab. Eng. 83, 183–192. https://doi.org/10.1016/j.ymben.2024.04.003.

Botstein, D., Fink, G.R., 2011. Yeast: an experimental organism for 21st Century biology. Genetics 189 (3), 695–704. https://doi.org/10.1534/genetics.111.130765.

Brandt, B.A., Garcia-Aparicio, M.D.P., Gorgens, J.F., van Zyl, W.H., 2021. Rational engineering of Saccharomyces cerevisiae towards improved tolerance to multiple inhibitors in lignocellulose fermentations. Biotechnol. Biofuels 14 (1), 173. https://doi.org/10.1186/s13068-021-02021-w.

Brennan, T.C., Kromer, J.O., Nielsen, L.K., 2013. Physiological and transcriptional responses of Saccharomyces cerevisiae to d-limonene show changes to the cell wall but not to the plasma membrane. Appl. Environ. Microbiol. 79 (12), 3590–3600. https://doi.org/10.1128/AEM.00463-13.

Brennan, T.C., Turner, C.D., Kromer, J.O., Nielsen, L.K., 2012. Alleviating monoterpene toxicity using a two-phase extractive fermentation for the bioproduction of jet fuel mixtures in Saccharomyces cerevisiae. Biotechnol. Bioeng. 109 (10), 2513–2522. https://doi.org/10.1002/bit.24536.

Cao, X., Yu, W., Chen, Y., Yang, S., Zhao, Z.K., Nielsen, J., Luan, H., Zhou, Y.J., 2023. Engineering yeast for high-level production of diterpenoid sclareol. Metab. Eng. 75, 19–28. https://doi.org/10.1016/j.ymben.2022.11.002.

Castano-Cerezo, S., Kulyk-Barbier, H., Millard, P., Portais, J.C., Heux, S., Truan, G., Bellvert, F., 2019. Functional analysis of isoprenoid precursors biosynthesis by quantitative metabolomics and isotopologue profiling. Metabolomics 15 (9), 115. https://doi.org/10.1007/s11306-019-1580-8.

Cautereels, C., Smets, J., Bircham, P., De Ruysscher, D., Zimmermann, A., De Rijk, P., Steensels, J., Gorkovskiy, A., Masschelein, J., Verstrepen, K.J., 2024a. Combinatorial optimization of gene expression through recombinase-mediated promoter and terminator shuffling in yeast. Nat. Commun. 15 (1), 1112. https://doi.org/10.1038/s41467-024-44997-7.

Cautereels, C., Smets, J., De Saeger, J., Cool, L., Zhu, Y., Zimmermann, A., Steensels, J., Gorkovskiy, A., Jacobs, T.B., Verstrepen, K.J., 2024b. Orthogonal LoxPsym sites allow multiplexed site-specific recombination in prokaryotic and eukaryotic hosts. Nat. Commun. 15 (1), 1113. https://doi.org/10.1038/s41467-024-44996-8.

Cheah, L.C., Liu, L., Stark, T., Plan, M.R., Peng, B., Lu, Z., Schenk, G., Sainsbury, F., Vickers, C.E., 2023. Metabolic flux enhancement from the translational fusion of terpene synthases is linked to terpene synthase accumulation. Metab. Eng. 77, 143–151. https://doi.org/10.1016/j.ymben.2023.03.012.

Chen, B., Lee, H.L., Heng, Y.C., Chua, N., Teo, W.S., Choi, W.J., Leong, S.S.J., Foo, J.L., Chang, M.W., 2018. Synthetic biology toolkits and applications in Saccharomyces cerevisiae. Biotechnol. Adv. 36 (7), 1870–1881. https://doi.org/10.1016/j.biotechadv.2018.07.005.

Chen, R., Jia, Q., Mu, X., Hu, B., Sun, X., Deng, Z., Chen, F., Bian, G., Liu, T., 2021. Systematic mining of fungal chimeric terpene synthases using an efficient precursor-providing yeast chassis. Proc. Natl. Acad. Sci. U. S. A. 118 (29). https://doi.org/10.1073/pnas.2023247118.

Cheng, S., Liu, X., Jiang, G., Wu, J., Zhang, J.L., Lei, D., Yuan, Y.J., Qiao, J., Zhao, G.R., 2019. Orthogonal engineering of biosynthetic pathway for efficient production of limonene in Saccharomyces cerevisiae. ACS Synth. Biol. 8 (5), 968–975. https://doi.org/10.1021/acssynbio.9b00135.

Cheng, S., Wang, X., Deng, Z., Liu, T., 2024. Innovative approaches in the discovery of terpenoid natural products. Curr. Opin. Microbiol. 83, 102575. https://doi.org/10.1016/j.mib.2024.102575.

Ciriminna, R., Lomeli-Rodriguez, M., Demma Cara, P., Lopez-Sanchez, J.A., Pagliaro, M., 2014. Limonene: a versatile chemical of the bioeconomy. Chem. Commun. 50 (97), 15288–15296. https://doi.org/10.1039/c4cc06147k.

Demissie, Z.A., Tarnowycz, M., Adal, A.M., Sarker, L.S., Mahmoud, S.S., 2019. A lavender ABC transporter confers resistance to monoterpene toxicity in yeast. Planta 249 (1), 139–144. https://doi.org/10.1007/s00425-018-3064-x.

Denby, C.M., Li, R.A., Vu, V.T., Costello, Z., Lin, W., Chan, L.J.G., Williams, J., Donaldson, B., Bamforth, C.W., Petzold, C.J., Scheller, H.V., Martin, H.G., Keasling, J.D., 2018. Industrial brewing yeast engineered for the production of primary flavor determinants in hopped beer. Nat. Commun. 9 (1), 965. https://doi.org/10.1038/s41467-018-03293-x.

Duperray, M., Delvenne, M., Francois, J.M., Delvigne, F., Capp, J.P., 2024. Genomic and metabolic instability during long-term fermentation of an industrial Saccharomyces cerevisiae strain engineered for C5 sugar utilization. Front. Bioeng. Biotechnol. 12, 1357671. https://doi.org/10.3389/fbioe.2024.1357671.

Dusseaux, S., Wajn, W.T., Liu, Y., Ignea, C., Kampranis, S.C., 2020. Transforming yeast peroxisomes into microfactories for the efficient production of high-value isoprenoids. Proc. Natl. Acad. Sci. U. S. A. 117 (50), 31789–31799. https://doi.org/10.1073/pnas.2013968117.

Feng, Q., Liu, Z.L., Weber, S.A., Li, S., 2018. Signature pathway expression of xylose utilization in the genetically engineered industrial yeast Saccharomyces cerevisiae. PLoS One 13 (4), e0195633. https://doi.org/10.1371/journal.pone.0195633.

Gallone, B., Steensels, J., Mertens, S., Dzialo, M.C., Gordon, J.L., Wauters, R., Thesseling, F.A., Bellinazzo, F., Saels, V., Herrera-Malaver, B., Prahl, T., White, C., Hutzler, M., Meussdoerffer, F., Malcorps, P., Souffriau, B., Daenen, L., Baele, G., Maere, S., Verstrepen, K.J., 2019. Interspecific hybridization facilitates niche adaptation in beer yeast. Nat Ecol Evol 3 (11), 1562–1575. https://doi.org/10.1038/s41559-019-0997-9.

Gallone, B., Steensels, J., Prahl, T., Soriaga, L., Saels, V., Herrera-Malaver, B., Merlevede, A., Roncoroni, M., Voordeckers, K., Miraglia, L., Teiling, C., Steffy, B., Taylor, M., Schwartz, A., Richardson, T., White, C., Baele, G., Maere, S., Verstrepen, K.J., 2016. Domestication and divergence of Saccharomyces cerevisiae beer yeasts. Cell 166 (6), 1397–1410. https://doi.org/10.1016/j.cell.2016.08.020 e1316.

Graef, M., 2018. Lipid droplet-mediated lipid and protein homeostasis in budding yeast. FEBS Lett. 592 (8), 1291–1303. https://doi.org/10.1002/1873-3468.12996.

Granchi, L., Ganucci, D., Buscioni, G., Mangani, S., Guerrini, S., 2019. The biodiversity of Saccharomyces cerevisiae in spontaneous wine fermentation: the occurrence and persistence of winery-strains. Fermentation 5 (4). https://doi.org/10.3390/fermentation5040086.

Hu, F., Liu, J., Du, G., Hua, Z., Zhou, J., Chen, J., 2012. Key cytomembrane ABC transporters of Saccharomyces cerevisiae fail to improve the tolerance to D-limonene. Biotechnol. Lett. 34 (8), 1505–1509. https://doi.org/10.1007/s10529-012-0931-6.

Hu, Z.C., Dai, H.W., Gu, B.Q., Wang, Y.S., Liu, Z.Q., Zheng, Y.G., 2025. The combination of ultraviolet mutagenesis and PPX1 overexpression synergistically enhanced S-adenosyl-L-methionine synthesis in industrial Saccharomyces cerevisiae. Enzym. Microb. Technol. 185, 110591. https://doi.org/10.1016/j.enzmictec.2025.110591.

Huang, Y., Ye, Z., Wan, X., Yao, G., Duan, J., Liu, J., Yao, M., Sun, X., Deng, Z., Shen, K., Jiang, H., Liu, T., 2023. Systematic mining and evaluation of the sesquiterpene skeletons as high energy aviation fuel molecules. Adv Sci (Weinh), e2300889. https://doi.org/10.1002/advs.202300889.

Ibanez, M.D., Sanchez-Ballester, N.M., Blazquez, M.A., 2020. Encapsulated limonene: a pleasant lemon-like aroma with promising application in the agri-food industry. A review. Molecules 25 (11). https://doi.org/10.3390/molecules25112598.

Ignea, C., Pontini, M., Maffei, M.E., Makris, A.M., Kampranis, S.C., 2014. Engineering monoterpene production in yeast using a synthetic dominant negative geranyl diphosphate synthase. ACS Synth. Biol. 3 (5), 298–306. https://doi.org/10.1021/sb400115e.

Ignea, C., Raadam, M.H., Motawia, M.S., Makris, A.M., Vickers, C.E., Kampranis, S.C., 2019. Orthogonal monoterpenoid biosynthesis in yeast constructed on an isomeric substrate. Nat. Commun. 10 (1), 3799. https://doi.org/10.1038/s41467-019-11290-x.

Jiang, G., Yao, M., Wang, Y., Xiao, W., Yuan, Y., 2021. A "push-pull-restrain" strategy to improve citronellol production in Saccharomyces cerevisiae. Metab. Eng. 66, 51–59. https://doi.org/10.1016/j.ymben.2021.03.019.

Jiang, G.Z., Yao, M.D., Wang, Y., Zhou, L., Song, T.Q., Liu, H., Xiao, W.H., Yuan, Y.J., 2017. Manipulation of GES and ERG20 for geraniol overproduction in Saccharomyces cerevisiae. Metab. Eng. 41, 57–66. https://doi.org/10.1016/j.ymben.2017.03.005.

Jongedijk, E., Cankar, K., Buchhaupt, M., Schrader, J., Bouwmeester, H., Beekwilder, J., 2016. Biotechnological production of limonene in microorganisms. Appl. Microbiol. Biotechnol. 100 (7), 2927–2938. https://doi.org/10.1007/s00253-016-7337-7.

Kong, I.I., Turner, T.L., Kim, H., Kim, S.R., Jin, Y.S., 2018. Phenotypic evaluation and characterization of 21 industrial Saccharomyces cerevisiae yeast strains. FEMS Yeast Res. 18 (1). https://doi.org/10.1093/femsyr/foy001.

Kong, X., Wu, Y., Yu, W., Liu, Y., Li, J., Du, G., Lv, X., Liu, L., 2023. Efficient synthesis of limonene in Saccharomyces cerevisiae using combinatorial metabolic engineering strategies. J. Agric. Food Chem. https://doi.org/10.1021/acs.jafc.3c02076.

Konzock, O., Nielsen, J., 2024. TRYing to evaluate production costs in microbial biotechnology. Trends Biotechnol. 42 (11), 1339–1347. https://doi.org/10.1016/j.tibtech.2024.04.007.

Leavell, M.D., McPhee, D.J., Paddon, C.J., 2016. Developing fermentative terpenoid production for commercial usage. Curr. Opin. Biotechnol. 37, 114–119. https://doi.org/10.1016/j.copbio.2015.10.007.

Li, D.X., Guo, Q., Yang, Y.X., Jiang, S.J., Ji, X.J., Ye, C., Wang, Y.T., Shi, T.Q., 2024. Recent advances and multiple strategies of monoterpenoid overproduction in Saccharomyces cerevisiae and Yarrowia lipolytica. ACS Synth. Biol. https://doi.org/10.1021/acssynbio.4c00297.

Liti, G., Carter, D.M., Moses, A.M., Warringer, J., Parts, L., James, S.A., Davey, R.P., Roberts, I.N., Burt, A., Koufopanou, V., Tsai, I.J., Bergman, C.M., Bensasson, D., O'Kelly, M.J., van Oudenaarden, A., Barton, D.B., Bailes, E., Nguyen, A.N., Jones, M., Louis, E.J., 2009. Population genomics of domestic and wild yeasts. Nature 458 (7236), 337–341. https://doi.org/10.1038/nature07743.

Liu, J., Zhu, Y., Du, G., Zhou, J., Chen, J., 2013. Response of Saccharomyces cerevisiae to D-limonene-induced oxidative stress. Appl. Microbiol. Biotechnol. 97 (14), 6467–6475. https://doi.org/10.1007/s00253-013-4931-9.

Liu, Y., Zhao, X., Gan, F., Chen, X., Deng, K., Crowe, S.A., Hudson, G.A., Belcher, M.S., Schmidt, M., Astolfi, M.C.T., Kosina, S.M., Pang, B., Shao, M., Yin, J., Sirirungruang, S., Iavarone, A.T., Reed, J., Martin, L.B.B., El-Demerdash, A., Keasling, J.D., 2024. Complete biosynthesis of QS-21 in engineered yeast. Nature 629 (8013), 937–944. https://doi.org/10.1038/s41586-024-07345-9.

Loegler, V., Friedrich, A., Schacherer, J., 2024. Overview of the Saccharomyces cerevisiae population structure through the lens of 3,034 genomes. G3 (Bethesda) 14 (12). https://doi.org/10.1093/g3journal/jkae245.

Luo, X., Reiter, M.A., d'Espaux, L., Wong, J., Denby, C.M., Lechner, A., Zhang, Y., Grzybowski, A.T., Harth, S., Lin, W., Lee, H., Yu, C., Shin, J., Deng, K., Benites, V.T., Wang, G., Baidoo, E.E.K., Chen, Y., Dev, I., Keasling, J.D., 2019. Complete biosynthesis of cannabinoids and their unnatural analogues in yeast. Nature 567 (7746), 123–126. https://doi.org/10.1038/s41586-019-0978-9.

Ma, Y., Zu, Y., Huang, S., Stephanopoulos, G., 2023. Engineering a universal and efficient platform for terpenoid synthesis in yeast. Proc. Natl. Acad. Sci. U. S. A. 120 (1), e2207680120. https://doi.org/10.1073/pnas.2207680120.

Madeira, F., Madhusoodanan, N., Lee, J., Eusebi, A., Niewielska, A., Tivey, A.R.N., Lopez, R., Butcher, S., 2024. The EMBL-EBI Job Dispatcher sequence analysis tools framework in 2024. Nucleic Acids Res. 52 (W1), W521–W525. https://doi.org/10.1093/nar/gkae241.

Mavrommati, M., Daskalaki, A., Papanikolaou, S., Aggelis, G., 2022. Adaptive laboratory evolution principles and applications in industrial biotechnology. Biotechnol. Adv. 54, 107795. https://doi.org/10.1016/j.biotechadv.2021.107795.

Meersman, E., Steensels, J., Mathawan, M., Wittocx, P.J., Saels, V., Struyf, N., Bernaert, H., Vrancken, G., Verstrepen, K.J., 2013. Detailed analysis of the microbial population in Malaysian spontaneous cocoa pulp fermentations reveals a core and variable microbiota. PLoS One 8 (12), e81559. https://doi.org/10.1371/journal.pone.0081559.

Meersman, E., Steensels, J., Struyf, N., Paulus, T., Saels, V., Mathawan, M., Allegaert, L., Vrancken, G., Verstrepen, K.J., Cullen, D., 2016. Tuning chocolate flavor through development of thermotolerant Saccharomyces cerevisiae starter cultures with increased acetate ester production. Appl. Environ. Microbiol. 82 (2), 732–746. https://doi.org/10.1128/aem.02556-15.

Miller, J.A., Thompson, P.A., Hakim, I.A., Chow, H.H.S., Thomson, C.A., 2010. d-Limonene: a bioactive food component from citrus and evidence for a potential role in breast cancer prevention and treatment. Oncol. Rev. 5 (1), 31–42. https://doi.org/10.1007/s12156-010-0066-8.

Monk, J.M., Koza, A., Campodonico, M.A., Machado, D., Seoane, J.M., Palsson, B.O., Herrgard, M.J., Feist, A.M., 2016. Multi-omics quantification of species variation of Escherichia coli links molecular features with strain phenotypes. Cell Syst. 3 (3), 238–251. https://doi.org/10.1016/j.cels.2016.08.013 e212.

Montano Lopez, J., Duran, L., Avalos, J.L., 2022. Physiological limitations and opportunities in microbial metabolic engineering. Nat. Rev. Microbiol. 20 (1), 35–48. https://doi.org/10.1038/s41579-021-00600-0.

Mukherjee, M., Blair, R.H., Wang, Z.Q., 2022. Machine-learning guided elucidation of contribution of individual steps in the mevalonate pathway and construction of a yeast platform strain for terpenoid production. Metab. Eng. 74, 139–149. https://doi.org/10.1016/j.ymben.2022.10.004.

Mukherjee, V., Steensels, J., Lievens, B., Van de Voorde, I., Verplaetse, A., Aerts, G., Willems, K.A., Thevelein, J.M., Verstrepen, K.J., Ruyters, S., 2014. Phenotypic evaluation of natural and industrial Saccharomyces yeasts for different traits desirable in industrial bioethanol production. Appl. Microbiol. Biotechnol. 98 (22), 9483–9498. https://doi.org/10.1007/s00253-014-6090-z.

Negro, V., Mancini, G., Ruggeri, B., Fino, D., 2016. Citrus waste as feedstock for bio-based products recovery: review on limonene case study and energy valorization. Bioresour. Technol. 214, 806–815. https://doi.org/10.1016/j.biortech.2016.05.006.

Olzmann, J.A., Carvalho, P., 2019. Dynamics and functions of lipid droplets. Nat. Rev. Mol. Cell Biol. 20 (3), 137–155. https://doi.org/10.1038/s41580-018-0085-z.

Paddon, C.J., Westfall, P.J., Pitera, D.J., Benjamin, K., Fisher, K., McPhee, D., Leavell, M. D., Tai, A., Main, A., Eng, D., Polichuk, D.R., Teoh, K.H., Reed, D.W., Treynor, T., Lenihan, J., Fleck, M., Bajad, S., Dang, G., Dengrove, D., Newman, J.D., 2013. High-level semi-synthetic production of the potent antimalarial artemisinin. Nature 496 (7446), 528–532. https://doi.org/10.1038/nature12051.

Paggiola, G., Stempvoort, S.V., Bustamante, J., Barbero, J.M.V., Hunt, A.J., Clark, J.H., 2016. Can bio-based chemicals meet demand? Global and regional case-study around citrus waste-derived limonene as a solvent for cleaning applications. Biofuel Bioprod. Biorefining 10 (6), 686–698. https://doi.org/10.1002/bbb.1677.

Pan, X., Yuan, D.S., Xiang, D., Wang, X., Sookhai-Mahadeo, S., Bader, J.S., Hieter, P., Spencer, F., Boeke, J.D., 2004. A robust toolkit for functional profiling of the yeast genome. Mol. Cell 16 (3), 487–496. https://doi.org/10.1016/j.molcel.2004.09.035.

Paramasivan, K., Mutturi, S., 2017. Regeneration of NADPH coupled with HMG-CoA reductase activity increases squalene synthesis in Saccharomyces cerevisiae. J. Agric. Food Chem. 65 (37), 8162–8170. https://doi.org/10.1021/acs.jafc.7b02945.

Peng, B., Esquirol, L., Lu, Z., Shen, Q., Cheah, L.C., Howard, C.B., Scott, C., Trau, M., Dumsday, G., Vickers, C.E., 2022. An in vivo gene amplification system for high level expression in Saccharomyces cerevisiae. Nat. Commun. 13 (1), 2895. https://doi.org/10.1038/s41467-022-30529-8.

Peng, B., Plan, M.R., Chrysanthopoulos, P., Hodson, M.P., Nielsen, L.K., Vickers, C.E., 2017. A squalene synthase protein degradation method for improved sesquiterpene production in Saccharomyces cerevisiae. Metab. Eng. 39, 209–219. https://doi.org/10.1016/j.ymben.2016.12.003.

Peter, J., De Chiara, M., Friedrich, A., Yue, J.X., Pflieger, D., Bergstrom, A., Sigwalt, A., Barre, B., Freel, K., Llored, A., Cruaud, C., Labadie, K., Aury, J.M., Istace, B., Lebrigand, K., Barbry, P., Engelen, S., Lemainque, A., Wincker, P., Schacherer, J., 2018. Genome evolution across 1,011 Saccharomyces cerevisiae isolates. Nature 556 (7701), 339–344. https://doi.org/10.1038/s41586-018-0030-5.

Rehm, B.H.A., Wibowo, D., 2022. Microbial Production of High-Value Products. Springer International Publishing. https://books.google.be/books?id=unGHEAAAQBAJ.

Reider Apel, A., d'Espaux, L., Wehrs, M., Sachs, D., Li, R.A., Tong, G.J., Garber, M., Nnadi, O., Zhuang, W., Hillson, N.J., Keasling, J.D., Mukhopadhyay, A., 2017. A Cas9-based toolkit to program gene expression in Saccharomyces cerevisiae. Nucleic Acids Res. 45 (1), 496–508. https://doi.org/10.1093/nar/gkw1023.

Ren, Y., Liu, S., Jin, G., Yang, X., Zhou, Y.J., 2020. Microbial production of limonene and its derivatives: achievements and perspectives. Biotechnol. Adv. 44, 107628. https://doi.org/10.1016/j.biotechadv.2020.107628.

Romano, P., Capece, A., Serafino, V., Romaniello, R., Poeta, C., 2008. Biodiversity of wild strains of Saccharomyces cerevisiae as tool to complement and optimize wine quality. World J. Microbiol. Biotechnol. 24 (9), 1797–1802. https://doi.org/10.1007/s11274-008-9672-z.

Shi, S., Ji, H., Siewers, V., Nielsen, J., 2016. Improved production of fatty acids by Saccharomyces cerevisiae through screening a cDNA library from the oleaginous

yeast Yarrowia lipolytica. FEMS Yeast Res. 16 (1), fov108. https://doi.org/10.1093/femsyr/fov108.
Siddiqui, M.S., Thodey, K., Trenchard, I., Smolke, C.D., 2012. Advancing secondary metabolite biosynthesis in yeast with synthetic biology tools. FEMS Yeast Res. 12 (2), 144–170. https://doi.org/10.1111/j.1567-1364.2011.00774.x.
Sitepu, I.R., Ignatia, L., Franz, A.K., Wong, D.M., Faulina, S.A., Tsui, M., Kanti, A., Boundy-Mills, K., 2012. An improved high-throughput Nile red fluorescence assay for estimating intracellular lipids in a variety of yeast species. J. Microbiol. Methods 91 (2), 321–328. https://doi.org/10.1016/j.mimet.2012.09.001.
Son, S.H., Kim, J.E., Moon, S.Y., Jang, I.S., Yu, B.J., Lee, J.Y., 2022. Metabolic recycling of storage lipids promotes squalene biosynthesis in yeast. Biotechnol Biofuels Bioprod 15 (1), 108. https://doi.org/10.1186/s13068-022-02208-9.
Steensels, J., Meersman, E., Snoek, T., Saels, V., Verstrepen, K.J., 2014a. Large-scale selection and breeding to generate industrial yeasts with superior aroma production. Appl. Environ. Microbiol. 80 (22), 6965–6975. https://doi.org/10.1128/AEM.02235-14.
Steensels, J., Snoek, T., Meersman, E., Picca Nicolino, M., Voordeckers, K., Verstrepen, K. J., 2014b. Improving industrial yeast strains: exploiting natural and artificial diversity. FEMS Microbiol. Rev. 38 (5), 947–995. https://doi.org/10.1111/1574-6976.12073.
Su, L., Liu, P., Liu, W., Liu, Q., Gao, J., Zhao, Q., Jia, K., Sheng, X., Ma, H., Wang, Q., Dai, Z., 2024. Computational design-enabled divergent modification of monoterpene synthases for terpenoid hyperproduction. ACS Catal. 17699–17715. https://doi.org/10.1021/acscatal.4c05863.
Sun, Z.J., Lian, J.Z., Zhu, L., Jiang, Y.Q., Li, G.S., Xue, H.L., Wu, M.B., Yang, L.R., Lin, J. P., 2021. Combined biosynthetic pathway engineering and storage pool expansion for high-level production of ergosterol in industrial Saccharomyces cerevisiae. Front. Bioeng. Biotechnol. 9, 681666. https://doi.org/10.3389/fbioe.2021.681666.
Thompson, J.R., Register, E., Curotto, J., Kurtz, M., Kelly, R., 1998. An improved protocol for the preparation of yeast cells for transformation by electroporation. Yeast 14 (6), 565–571. https://doi.org/10.1002/(sici)1097-0061(19980430)14:6<565::Aid-yea251>3.0.Co;2-b.
Vieira, A.J., Beserra, F.P., Souza, M.C., Totti, B.M., Rozza, A.L., 2018. Limonene: aroma of innovation in health and disease. Chem. Biol. Interact. 283, 97–106. https://doi.org/10.1016/j.cbi.2018.02.007.
Wan, Z., Hu, H., Liu, K., Qiao, Y., Guo, F., Wang, C., Xin, F., Zhang, W., Jiang, M., 2024. Engineering industrial yeast for improved tolerance and robustness. Crit. Rev. Biotechnol. 44 (8), 1461–1477. https://doi.org/10.1080/07388551.2024.2326677.
Wang, S., Zhan, C., Nie, S., Tian, D., Lu, J., Wen, M., Qiao, J., Zhu, H., Caiyin, Q., 2023. Enzyme and metabolic engineering strategies for biosynthesis of alpha-farnesene in Saccharomyces cerevisiae. J. Agric. Food Chem. 71 (33), 12452–12461. https://doi.org/10.1021/acs.jafc.3c03677.
Wei, L.J., Kwak, S., Liu, J.J., Lane, S., Hua, Q., Kweon, D.H., Jin, Y.S., 2018. Improved squalene production through increasing lipid contents in Saccharomyces cerevisiae. Biotechnol. Bioeng. 115 (7), 1793–1800. https://doi.org/10.1002/bit.26595.
Welte, M.A., Gould, A.P., 2017. Lipid droplet functions beyond energy storage. Biochim. Biophys. Acta Mol. Cell Biol. Lipids 1862 (10 Pt B), 1260–1272. https://doi.org/10.1016/j.bbalip.2017.07.006.
Westfall, P.J., Pitera, D.J., Lenihan, J.R., Eng, D., Woolard, F.X., Regentin, R., Horning, T., Tsuruta, H., Melis, D.J., Owens, A., Fickes, S., Diola, D., Benjamin, K.R., Keasling, J.D., Leavell, M.D., McPhee, D.J., Renninger, N.S., Newman, J.D., Paddon, C.J., 2012. Production of amorphadiene in yeast, and its conversion to dihydroartemisinic acid, precursor to the antimalarial agent artemisinin. Proc. Natl. Acad. Sci. U. S. A. 109 (3), E111–118. https://doi.org/10.1073/pnas.1110740109.
Zhang, J., Hansen, L.G., Gudich, O., Viehrig, K., Lassen, L.M.M., Schrubbers, L., Adhikari, K.B., Rubaszka, P., Carrasquer-Alvarez, E., Chen, L., D'Ambrosio, V., Lehka, B., Haidar, A.K., Nallapareddy, S., Giannakou, K., Laloux, M., Arsovska, D., Jorgensen, M.A.K., Chan, L.J.G., Keasling, J.D., 2022. A microbial supply chain for production of the anti-cancer drug vinblastine. Nature 609 (7926), 341–347. https://doi.org/10.1038/s41586-022-05157-3.
Zhang, X., Liu, X., Meng, Y., Zhang, L., Qiao, J., Zhao, G.-R., 2021. Combinatorial engineering of Saccharomyces cerevisiae for improving limonene production. Biochem. Eng. J. 176. https://doi.org/10.1016/j.bej.2021.108155.
Zhou, P., Zhou, X., Yuan, D., Fang, X., Pang, X., Yuan, K., Li, A., Wang, X., 2023. Combining protein and organelle engineering for linalool overproduction in Saccharomyces cerevisiae. J. Agric. Food Chem. 71 (26), 10133–10143. https://doi.org/10.1021/acs.jafc.2c08416.
Zimmermann, A., Prieto-Vivas, J.E., Cautereels, C., Gorkovskiy, A., Steensels, J., Van de Peer, Y., Verstrepen, K.J., 2023. A Cas3-base editing tool for targetable in vivo mutagenesis. Nat. Commun. 14 (1). https://doi.org/10.1038/s41467-023-39087-z.
Zimmermann, A., Prieto-Vivas, J.E., Voordeckers, K., Bi, C., Verstrepen, K.J., 2024. Mutagenesis techniques for evolutionary engineering of microbes - exploiting CRISPR-Cas, oligonucleotides, recombinases, and polymerases. Trends Microbiol. https://doi.org/10.1016/j.tim.2024.02.006.